electronic reprint

STRUCTURAL CHEMISTRY

ISSN: 2053-2296
journals.iucr.org/c

Crystallographic and computational study of a network composed of $[ZnCl_4]^{2-}$ anions and triply protonated 4′-functionalized terpyridine cations

Juan Granifo, Sebastián Suárez, Fernando Boubeta and Ricardo Baggio

Acta Cryst. (2017). C**73**, 1121–1130

Acta Cryst C STRUCTURAL CHEMISTRY
ISSN 2053-2296

Crystallographic and computational study of a network composed of $[ZnCl_4]^{2-}$ anions and triply protonated 4′-functionalized terpyridine cations

Juan Granifo,[a]‡ Sebastián Suárez,[b]* Fernando Boubeta[b] and Ricardo Baggio[c]*

[a]Departamento de Ciencias Químicas y Recursos Naturales, Facultad de Ingeniería y Ciencias, Universidad de La Frontera, Casilla 54-D, Temuco, Chile, [b]Departamento de Química Inorgánica, Analítica y Química, Física/INQUIMAE–CONICET, Facultad de Ciencias Exactas y Naturales, Universidad de Buenos Aires, Buenos Aires, Argentina, and [c]Gerencia de Investigación y Aplicaciones, Centro Atómico Constituyentes, Comisión Nacional de Energía Atómica, Buenos Aires, Argentina. *Correspondence e-mail: seba@qi.fcen.uba.ar, baggio@tandar.cnea.gov.ar

Received 29 September 2017
Accepted 12 November 2017

Edited by D. R. Turner, University of Monash, Australia

‡ Author to whom enquires should be addressed, at juan.granifo@ufrontera.cl

Keywords: terpyridine; crystal structure; anion···π interactions; Hirshfeld surfaces; enrichment ratio; AIM analysis; computational chemistry.

CCDC reference: 1585155

Supporting information: this article has supporting information at journals.iucr.org/c

We report herein the synthesis, crystallographic analysis and a study of the noncovalent interactions observed in the new 4′-substituted terpyridine-based derivative bis[4′-(isoquinolin-2-ium-4-yl)-2,2′:6′,2″-terpyridine-1,1″-diium] tris-[tetrachloridozincate(II)] monohydrate, $(C_{24}H_{19}N_4)_2[ZnCl_4]_3{\cdot}H_2O$ or $(ITPH_3)_2$-$[ZnCl_4]_3{\cdot}H_2O$, where $(ITPH_3)^{3+}$ is the triply protonated cation derived from 4′-(isoquinolin-4-yl)-2,2′:6′,2″-terpyridine (ITP) [Granifo *et al.* (2016). *Acta Cryst.* C**72**, 932–938]. The $(ITPH_3)^{3+}$ cation presents a number of interesting similarities and differences compared with its neutral ITP relative, mainly in the role fulfilled in the packing arrangement by the profuse set of D—H···A [D (donor) = C, N or O; A (acceptor) = O or Cl], π–π and anion···π noncovalent interactions present. We discuss these interactions in two different complementary ways, *viz.* using a point-to-point approach in the light of Bader's theory of Atoms In Molecules (AIM), analyzing the individual significance of each interaction, and in a more 'global' analysis, making use of the Hirshfeld surfaces and the associated enrichment ratio (ER) approach, evaluating the surprisingly large co-operative effect of the superabundant weaker contacts.

1. Introduction

A few structural and solid-state theoretical studies on the noncovalent interactions in crystals containing protonated 4′-pyridyl-substituted terpyridines have been carried out in the last few years (Padhi *et al.*, 2011; Seth *et al.*, 2013; Manna *et al.*, 2013, 2014*a*,*b*). These species have been obtained from the reaction of the free bases L [L = 4′-(pyridin-4-yl)-2,2′:6′,2″-terpyridine, 4′-(pyridin-2-yl)-2,2′:6′,2′-terpyridine and 4′-(pyridin-4-yl)-3,2′:6′,3″-terpyridine] with inorganic acids (HNO_3, HBr and $HClO_4$), giving rise, in each case, to one triply protonated LH_3^{3+} cation. It was observed that only the N atoms of the three outermost pyridyl groups are protonated and that the lateral rings of the terpyridine portion adopt a *syn–syn* conformation with respect to the central pyridine ring. The analysis of the noncovalent interactions disclosed the pivotal role that anion···π interactions play in the final stabilization of the crystal packing, through its concerted action with the hydrogen bonding and the π–π stacking interactions. In this latter case, it was concluded that they are enhanced if the π-system is charged, in spite of the repulsive electrostatic nature between positively charged LH_3^{3+} cations (Seth *et al.*, 2013; Manna *et al.*, 2013). Thus, a variety of interactions between the charged aromatic rings and the different anions were described as a series of intricate

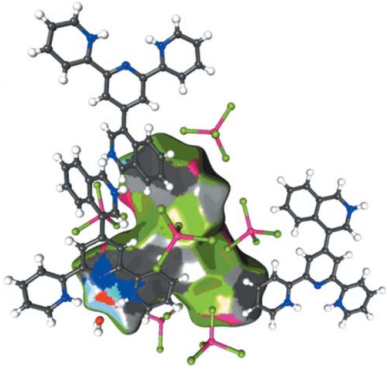

networks, *i.e.* anion···π···anion, anion···π–π and anion···π–π···anion (Manna *et al.*, 2014*a*,*b*).

Herein, as an extension of these studies on protonated 4′-functionalized terpyridine derivatives, we have selected as the starting neutral base an N-containing fused-ring system whose crystal and molecular structure we have reported recently, *viz.* 4′-(isoquinolin-4-yl)-2,2′:6′,2″-terpyridine (ITP), (**I**) (see Scheme; Granifo *et al.*, 2016). By mixing (**I**) with zinc chloride and hydrochloric acid, crystals of the new tetrachlorozincate salt $(ITPH_3)_2[ZnCl_4]_3\cdot H_2O$, (**II**) (see Scheme), containing the triply protonated $(ITPH_3)^{3+}$ cation, were successfully isolated. The $(ITPH_3)^{3+}$ cation in (**II**) presents a number of interesting similarities and differences compared with (**I**), which we shall discuss in detail, mainly with regard to the role fulfilled in the packing arrangement by the profuse set of D—H···A [D (donor) = C, N or O; A (acceptor) = O or Cl], π–π and anion···π noncovalent interactions present. We shall discuss the latter in two different complementary ways, *viz.* using a quantitave point-to-point approach in the light of Bader's theory of Atoms In Molecules (AIM; Bader, 1990, 2009) and in a more 'global' analysis, making use of the Hirshfeld surfaces (Spackman & Byrom, 1997) and the associated, recently developed, enrichment ratio (ER) approach (Jelsch *et al.*, 2014).

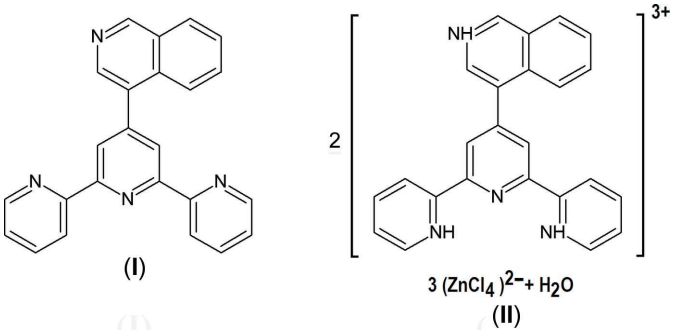

2. Experimental

IR spectra were recorded on a Bruker Tensor 27 FT–IR spectrometer (using KBr plates) or an Agilent Cary 630 FT–IR spectrometer using a Diamond ATR (attenuated total reflectance) accessory. X-ray diffraction data were collected with an Oxford Diffraction Xcalibur CCD Eos Gemini diffractometer with graphite-monochromated Mo $K\alpha$ radiation.

2.1. Synthesis and crystallization

The title tetrachloridozincate salt $(ITPH_3)_2[ZnCl_4]_3\cdot H_2O$ was prepared by the reaction of 4′-(isoquinolin-4-yl)-2,2′:6′,2″-terpyridine (ITP; Granifo *et al.*, 2016), $ZnCl_2$ and concentrated HCl (37%). ITP (4.3 mg, 0.012 mmol) was placed in a small beaker and dissolved with concentrated HCl (0.5 ml). To this solution was added an excess of $ZnCl_2$ (42.0 mg, 0.31 mmol) and the resulting solution was stirred for 1 min. The clear solution was allowed to stand at room temperature for 14 h to give colourless block-shaped crystals, which were washed with methanol (2 × 1 ml) and then dried in air (yield 7.0 mg, 86%). Analysis calculated for $C_{48}H_{40}Cl_{12}N_8OZn_3$: C 42.19, H 2.95, N 8.20%; found: C 42.22, H 2.98, N 8.19%. ATR FT–IR (cm^{-1}): 3172 (*w*), 3146 (*w*), 3082 (*w*), 3059 (*w*), 1600 (*s*), 1527 (*s*), 1418 (*m*), 1388 (*m*), 1347 (*m*), 1293 (*m*), 1238 (*s*), 1157 (*m*), 1098 (*w*), 1064 (*w*), 1042 (*m*), 992 (*m*), 916 (*w*), 873 (*m*), 834 (*s*), 782 (*s*), 769 (*m*), 744 (*m*), 726 (*m*), 626 (*m*), 618 (*s*).

Table 1
Experimental details.

Crystal data	
Chemical formula	$(C_{24}H_{19}N_4)_2[ZnCl_4]_3\cdot H_2O$
M_r	1366.39
Crystal system, space group	Triclinic, $P\overline{1}$
Temperature (K)	150
a, b, c (Å)	11.0485 (6), 16.0249 (8), 16.4318 (7)
α, β, γ (°)	100.824 (4), 103.574 (4), 102.737 (4)
V (Å^3)	2668.9 (2)
Z	2
Radiation type	Mo $K\alpha$
μ (mm^{-1})	1.98
Crystal size (mm)	0.30 × 0.25 × 0.20
Data collection	
Diffractometer	Rigaku Xcalibur Sapphire3
Absorption correction	Multi-scan (*CrysAlis PRO*; Rigaku Oxford Diffraction, 2015)
T_{min}, T_{max}	0.54, 0.70
No. of measured, independent and observed [$I > 2\sigma(I)$] reflections	29335, 12387, 9230
R_{int}	0.049
(sin $\theta/\lambda)_{max}$ (Å^{-1})	0.681
Refinement	
$R[F^2 > 2\sigma(F^2)]$, $wR(F^2)$, S	0.043, 0.092, 0.93
No. of reflections	12387
No. of parameters	673
No. of restraints	9
H-atom treatment	H atoms treated by a mixture of independent and constrained refinement
$\Delta\rho_{max}$, $\Delta\rho_{min}$ (e Å^{-3})	0.66, −0.48

Computer programs: *CrysAlis PRO* (Rigaku Oxford Diffraction, 2015), *SHELXS97* (Sheldrick, 2008), *SHELXTL* (Sheldrick, 2008), *Mercury* (Bruno *et al.*, 2002), *SHELXL2014* (Sheldrick, 2015) and *PLATON* (Spek, 2009).

2.2. Refinement

The crystal data, solution and refinement parameters are listed in Table 1. The good quality of the low-temperature data set allowed a clear distinction to be made between the intervening atomic species (C and N) originally in the difference maps and those later confirmed by the refinement of their displacement factors and the hydrogen-bonding interaction scheme. H atoms were identified in an intermediate difference map and treated differently in the refinement. Those attached to C atoms were further idealized and finally allowed to ride, with C—H = 0.93 Å, and with displacement parameters taken as $U_{iso}(H) = 1.2U_{eq}(C)$. Those attached to N atoms were refined with restrained N—H = 0.85 (1) Å and $U_{iso}(H) = 1.2U_{eq}(N)$, while water H atoms were restrained to have O—H = 0.90 (1) Å, H···H = 1.41 (2) Å and $U_{iso}(H) = 1.5U_{eq}(O)$.

2.3. Hirshfeld surface and enrichment ratio (ER) analysis

The three-dimensional Hirshfeld surfaces (Spackman & Byrom, 1997) were used to visualize and analyze the inter-

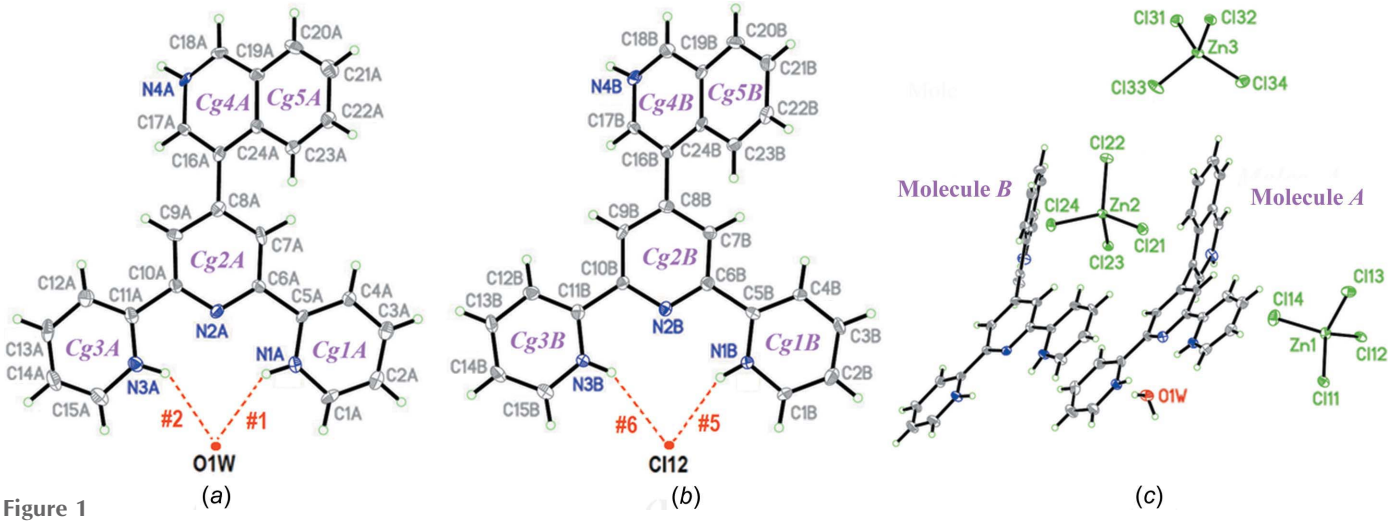

Figure 1
Molecular views of the molecules in (**II**), with displacement ellipsoids drawn at the 50% probability level, showing (*a*) molecule *A*, (*b*) molecule *B* and (*c*) the whole asymmetric unit (the #*n* interaction codes are as in Table 3).

Table 2
Relevant dihedral angles (°) between pyridine rings in (**II**).

<*Cg*–*Cg*>	(**II***A*)	(**II***B*)
<*Cg*2–*Cg*1>	4.6 (2)	3.1 (2)
<*Cg*2–*Cg*3>	6.6 (2)	6.6 (2)
<*Cg*2–*Cg*4>	46.7 (2)	42.2 (2)
<*Cg*2–*Cg*5>	47.7 (2)	44.7 (2)
<*Cg*4–*Cg*5>	2.5 (2)	1.6 (2)

molecular interactions, which were, in turn, evaluated using the recently introduced enrichment ratio (ER) approach (Jelsch *et al.*, 2014). Calculations were made with the *MoProViewer* software (Guillot, 2011). (General remarks on Hirshfeld surfaces are presented in the supporting information.)

2.4. Quantum mechanical calculations and Atoms In Molecules (AIM) analysis

Quantum mechanical calculations were performed using the hybrid exchange-correlation functional of Perdew, Burke and Ernzerhof (PBE) (Perdew *et al.*, 1996, 1997) with the Grimme's Dispersion correction (D3) for the van der Waals (VdW) energy (Grimme *et al.*, 2010). The 6-311++G(d,p) basis set was used for nonmetallic atoms. LanL2DZ (Hay & Wadt, 1985), along with its effective core potentials, was used as the basis set for the core electrons of the Zn atoms and 6-311++G(d,p) was used for the noncore electrons (Yang *et al.*, 2009; Yarwood *et al.*, 2009). All of the single-point calculations were performed using the *GAUSSIAN03* program (Frisch *et al.*, 2009), starting from the crystallographic atomic coordinates. The basis set superposition error (BSSE) for the calculation of interaction energies was corrected using the counterpoise method. The AIM analysis of the electron density was performed at the same level of theory using the *Multiwfn* program (Lu & Chen, 2012). The density functional theory (DFT) test case study was performed in a similar manner to AIM[1], but with previous optimizations of the system.

3. Results and discussion

3.1. Structure description

The title compound, (**II**), crystallizes in the space group $P\overline{1}$ and its crystal and molecular structure were determined by single-crystal X-ray diffraction. Relevant experimental data is presented in Table 1, while Fig. 1 shows the molecular geometry, as well as the atom and ring labelling. There are two independent $(ITPH_3)^{3+}$ cations (*A* and *B*), protonated at atoms N1 and N3 in the lateral pyridine rings (hereinfter py) and at N4 of the isoquinoline group (hereinafter isq). Charge balance is achieved by three independent $[ZnCl_4]^{2-}$ (tcz) anions and the asymmetric unit is completed by one hydration water molecule. As frequently happens in cases with multiple moieties in the asymmetric unit, there is some kind of frustrated symmetry linking independent molecules. In the present case, this is of a translational type; the application of a (0.22228, −0.31704, −0.15938) shift to cation *A* leads to a nearly overlapping disposition of all the atoms in the *A* and *B* units (see the supporting information).

The bond lengths and angles are unremarkable in both $(ITPH_3)^{3+}$ cations, the most relevant features coming from the dihedral angles involving the internal planar groups. Even if slightly deformed, the terpyridine nucleus (hereinafter tpy) can be considered to be basically planar, as assessed by the small interplanar angles between the py rings presented in Table 2. The isq groups, in contrast, are rotated significantly out of the tpy least-squares planes (see the <*Cg*2–*Cg*4> and <*Cg*2–*Cg*5> angles in Table 2). This large deviation is needed

[1] AIM (an acronym for the 'Atoms In Molecules' theory; Bader, 1990, 2009) interprets chemical bonding in terms of shared or closed-shell interactions, characterized by the electron density [$\rho(r)$], its gradient vector [$\nabla\rho(r)$] and its Laplacian [$\nabla^2\rho(r)$] at particular points termed 'Bond Critical Points', where the sign and magnitude of $\rho(r)$ and $\nabla^2\rho(r)$ define the interaction type.

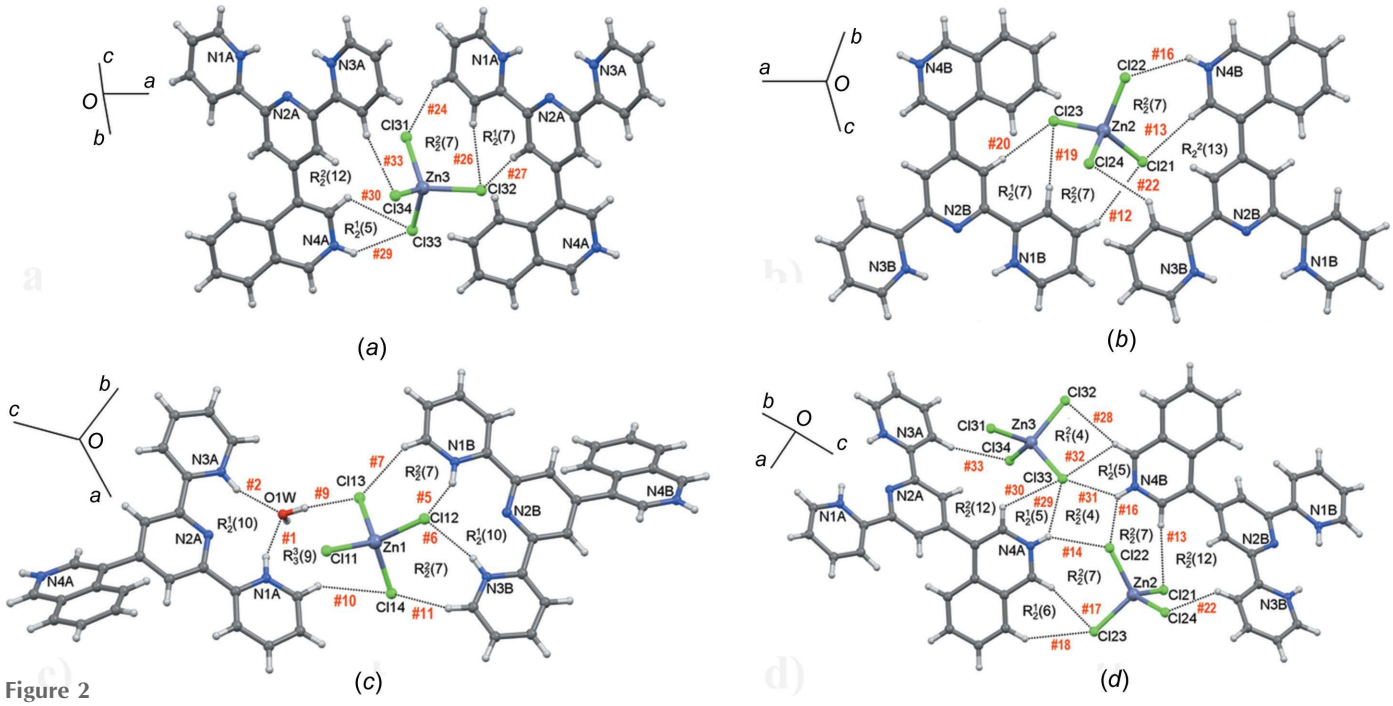

Figure 2
A few 'snapshots' showing the tetrachloridozincate bridging modes in (**II**), as well as the graph-set codes of the rings formed. (*a*) Zn3, bridging type *A* molecules, (*b*) Zn2, bridging type *B* molecules, (*c*) Zn1, bridging type *A*–type *B* molecules, and (*d*) Zn2—Zn3, bridging type *A*–type *B* molecules.

Table 3
Hydrogen-bond geometry (Å, °) in (**II**).

To facilitate the packing description, these interactions have been described with the acceptor at the 'reference site', the symmetry operations being applied to the *X*—H donor (*X* = O, N or C).

Code	*D*—H···*A*	*D*—H	H···*A*	*D*···*A*	*D*—H···*A*	100$\rho(r)$ (a.u.)	10$\nabla^2\rho(r)$ (a.u.)
#1	(N1*A*—H1*NA*)···O1*W*	0.85 (1)	1.95 (2)	2.769 (4)	161 (3)	2.59	0.66
#2	(N3*A*—H3*NA*)···O1*W*	0.85 (1)	1.95 (2)	2.753 (4)	158 (3)	2.64	1.08
#3	(C14*A*—H14*A*)^{i}···Cl11	0.93	2.62	3.440 (4)	148	1.15	0.38
#4	(C2*B*—H2*B*)^{ii}···Cl11	0.93	2.59	3.370 (4)	142	1.22	0.42
#5	(N1*B*—H1*NB*)^{iii}···Cl12	0.85 (1)	2.30 (2)	3.053 (3)	148 (3)	2.09	0.72
#6	(N3*B*—H3*NB*)^{iii}···Cl12	0.85 (1)	2.51 (2)	3.274 (3)	151 (3)	1.35	0.45
#7	(C1*B*—H1*B*)^{iii}···Cl13	0.93	2.79	3.342 (3)	119	0.83	0.24
#8	(C2*B*—H2*B*)^{ii}···Cl13	0.93	2.90	3.564 (3)	130	0.80	0.22
#9	(O1*W*—H1*WB*)^{ii}···Cl13	0.89 (1)	2.18 (1)	3.071 (3)	173 (3)	2.71	0.66
#10	(C1*A*—H1*A*)^{ii}···Cl14	0.93	2.80	3.467 (3)	129	0.87	0.25
#11	(C15*B*—H15*B*)^{iii}···Cl14	0.93	2.94	3.518 (4)	121	0.89	0.24
#12	(C3*B*—H3*B*)···Cl21	0.93	2.93	3.756 (3)	150	0.90	0.25
#13	(C17*B*—H17*B*)^{iv}···Cl21	0.93	2.77	3.690 (3)	173	0.84	0.25
#14	(N4*A*—H4*NA*)^{v}···Cl22	0.85 (1)	2.64 (2)	3.358 (3)	143 (3)	0.98	0.35
#15	(C18*A*—H18*A*)^{v}···Cl22	0.93	3.00	3.536 (4)	118	0.64	0.22
#16	(N4*B*—H4*NB*)^{iv}···Cl22	0.85 (1)	2.69 (3)	3.273 (3)	127 (3)	0.96	0.34
#17	(C18*A*—H18*A*)^{v}···Cl23	0.93	2.63	3.503 (3)	156	1.08	0.35
#18	(C20*A*—H20*A*)^{v}···Cl23	0.93	2.95	3.737 (4)	144	0.94	0.30
#19	(C4*B*—H4*B*)···Cl23	0.93	2.65	3.559 (3)	167	1.05	0.40
#20	(C7*B*—H7*B*)···Cl23	0.93	2.69	3.620 (3)	175	0.97	0.35
#21	(C4*B*—H4*B*)···Cl24	0.93	2.96	3.382 (3)	110	0.82	0.27
#22	(C12*B*—H12*B*)^{iv}···Cl24	0.93	2.74	3.461 (3)	135	0.94	0.30
#23	(C2*A*—H2*A*)^{vi}···Cl31	0.93	2.88	3.636 (4)	140	0.83	0.24
#24	(C3*A*—H3*A*)^{viii}···Cl31	0.93	2.80	3.620 (4)	147	0.84	0.25
#25	(O1*W*—H1*WA*)^{vii}···Cl32	0.89 (1)	2.17 (1)	3.044 (2)	166 (3)	2.65	0.62
#26	(C4*A*—H4*A*)^{viii}···Cl32	0.93	2.90	3.808 (3)	165	0.83	0.25
#27	(C7*A*—H7*A*)^{viii}···Cl32	0.93	2.70	3.612 (3)	166	0.85	0.26
#28	(C18*B*—H18*B*)^{iv}···Cl32	0.93	2.88	3.757 (3)	158	0.66	0.19
#29	(N4*A*—H4*NA*)^{v}···Cl33	0.85 (1)	2.57 (3)	3.159 (3)	127 (3)	1.24	0.47
#30	(C17*A*—H17*A*)^{v}···Cl33	0.93	2.83	3.324 (3)	114	0.93	0.33
#31	(N4*B*—H4*NB*)^{iv}···Cl33	0.85 (1)	2.55 (3)	3.181 (3)	133 (3)	1.23	0.47
#32	(C18*B*—H18*B*)^{iv}···Cl33	0.93	2.75	3.292 (4)	118	1.02	0.37
#33	(C12*A*—H12*A*)^{v}···Cl34	0.93	2.62	3.526 (4)	165	0.59	0.17

Symmetry codes: (i) $-x+2, -y+1, -z+2$; (ii) $-x+1, -y+1, -z+2$; (iii) $x, y+1, z$; (iv) $x-1, y, z$; (v) $-x+1, -y+1, -z+1$; (vi) $x, y, z-1$; (vii) $x-1, y, z-1$; (viii) $-x, -y+1, -z+1$.

Table 4
π–π contacts in (**II**).

The ring codes are as in Fig. 1. ccd is the centre-to-centre distance, da is the dihedral angle between rings, sa is the slippage angle and ipd is the interplanar distance, or (mean) distance from one plane to the neighbouring centroid. For details, see Janiak (2000).

Interaction code	$Cg\cdots Cg$	ccd (Å)	da (°)	sa (°)	ipd (Å)	$100\rho(r)$ (a.u.)	$10\nabla^2\rho(r)$ (a.u.)
#34	$Cg1A\cdots Cg2A^{ii}$	3.6718 (18)	4.28 (15)	24 (2)	3.35 (5)	0.58	0.17
#35	$Cg4A\cdots Cg5A^{i}$	3.8686 (19)	2.74 (15)	24.8 (15)	3.50 (4)	0.52	0.16
#36	$Cg3A\cdots Cg1B$	3.7397 (19)	3.96 (15)	28 (1)	3.30 (3)	0.55	0.16

Symmetry codes: (i) $-x+1, -y+1, -z+1$; (ii) $-x+1, -y+1, -z+2$.

Table 5
Anion$\cdots\pi$ (to *Cg*2 and *Cg*5) and anion$\cdots\pi^+$ (to *Cg*1 and *Cg*3) interactions in (**II**).

d is the Cl$\cdots X$ distance (Å), where *X* is the atom in the ring which lies nearest the Cl^- anion; α is the angle subtended by the Cl–*Cg* vector to the ring normal (°); β is the angle subtended by the *X*–*Cg* and *X*–Cl vectors (°) ($\beta < 90°$ = the anion projects within the ring; $90° < \beta$ = anion projects outside the ring); *n* (in η^n) is the number of interacting atoms. *N.b.* according to standard requirements for anion$\cdots\pi$ interactions (Gamez, 2014; Giese *et al.*, 2015; Bauza *et al.*, 2016), β should be < 100°. However, see interaction #42, ranked by AIM as the strongest among the anion$\cdots\pi$ interactions.

Code	Zn—Cl$\cdots Cg$	Cl$\cdots Cg$ (Å)	*d* (Å)	α (°)	β (°)	η^n	$100\rho(r)$ (a.u.)	$10\nabla^2\rho(r)$ (a.u.)
#37	Zn1—Cl11$\cdots Cg3B^{v}$	3.449	3.358	15.10	82.3	η^4	0.93	0.29
#38	Zn1—Cl11$\cdots Cg1A^{ii}$	3.746	3.324	28.65	97.1	η^3	0.95	0.31
#39	Zn2—Cl22$\cdots Cg3B^{ix}$	3.741	3.739	11.01	79.8	η^2	0.43	0.12
#40	Zn2—Cl23$\cdots Cg2A$	3.764	3.292	33.82	98.9	η^2	0.94	0.29
#41	Zn2—Cl23$\cdots Cg5B$	3.843	3.461	27.01	95.3	η^3	0.67	0.20
#42	Zn2—Cl24$\cdots Cg2B^{ix}$	3.838	3.275	37.42	104.5	η^2	0.97	0.28
#43	Zn3—Cl31$\cdots Cg3A^{i}$	3.776	3.427	32.24	94.4	η^2	0.86	0.23
#44	Zn3—Cl32$\cdots Cg5A^{iv}$	3.650	3.410	21.52	88.7	η^3	0.83	0.22

Symmetry codes: (i) $-x+1, -y+1, -z+1$; (ii) $-x+1, -y+1, -z+2$; (iv) $-x, -y+1, -z+1$; (v) $-x+2, -y+1, -z+2$; (ix) $-x+1, -y, -z+1$.

to avoid 'bumping' between atoms H7 and H23. The experimental H7$\cdots$H23 distance lies in the range 2.30–2.35 Å, while in a perfectly planar disposition, this value would collapse down to $\simeq$0.80 Å. This 'antibumping' argument appears to be reinforced by the difference between the angles centred at C16*A* and C16*B* (C24—C16—C8 > C17—C16—C8), suggesting some kind of H7$\cdots$H23 repulsion. However, an absolutely analogous situation was found in the close relative (**I**), and, in this case, a careful AIM analysis showed the H$\cdots$H interaction to be attractive instead.

Even if the previously reported structure of (**I**) and that of the present (**II**) are very similar in their bond lengths and angles, there is a striking difference in the disposition of py groups 1 and 3, which in unprotonated (**I**) has the corresponding py atoms N1 and N3 *anti* to N2 of the central ring, while in both independent molecules in (**II**), they are *syn* and involved in hydrogen bonding. It is relevant to mention that a search in the Cambridge Structural Database (CSD, Version 5.38; Groom *et al.*, 2016) for similarly protonated tpy units revealed 45 hits which presented the lateral py rings in a disposition similar to that in (**II**), with atoms N1 and N3 *syn* to N2 (denoted group 1), and only one in a *anti* mode (group 2). All of them presented their N—H groups strongly involved in hydrogen bonding, most of the interactions in group 1 being directed towards one single central acceptor, as in (**II**), and that in group 2 (CSD refcode KUCRUX; Chen *et al.*, 2015) making hydrogen bonds to two lateral ClO_4^- anions.

The most conspicuous aspect of structure (**II**) is its packing scheme, derived from a pletora of different intermolecular interactions (N—H$\cdots$Cl, N—H$\cdots$O, C—H$\cdots$Cl, Zn—Cl$\cdots\pi$ and π–π) presented in Tables 3 (hydrogen bonds), 4 (π–π interactions) and 5 (anion$\cdots\pi$ interactions), which for convenience of description have been assigned an individual 'code' or sequence number (from #1 to #44).

The large number of donors (six N—H, two O—H and many weaker C—H groups), as well as acceptors (12 Cl + 1 O), make hydrogen bonding the most abundant noncovalent interaction in the structure. The result is an extremely complex interaction scheme, where all the aforementioned agents are actively involved, in the form of an intricate interlinkage of two 'donor' groups (cation *A*, plus the strongly attached water solvent, and cation *B*) and three 'acceptor' nodes, *i.e.* the tcz groups, which for simplicity we will denote by their central Zn atom, Zn1, Zn2 and Zn3. Each of these acceptors acts as a connector linking a large number of donors (*viz.* Zn1 and Zn3 connect five molecules each, while Zn2 connects four molecules). Table 3 gives a full quantitative account of the 33 hydrogen-bonding interactions involved, but a clearer insight can be grasped from the 'snapshots' of the denser interactive regions given in Fig. 2, where a selection of relevant hydrogen bonds is given, as well as the graph-set codes for the rings to which these chelating interactions give rise. Figs. 2(*a*) and 2(*b*) disclose the way in which atoms Zn3 and Zn2 link molecules of a similar type (*A* and *B*, respectively). Similarly, Figs. 2(*c*) and 2(*d*) clarify the linkage of different molecular types *via* Zn1 (Fig. 2*c*) and Zn2–Zn3 (Fig. 2*d*). Complementing these partial views, Fig. 3 presents a combined version of Figs. 2(*c*) and 2(*d*), showing the collective bridging action of all three tcz moieties in the $[11\bar{1}]$ direction.

One further point which confirms the exceptional character of (**II**) with regard to noncovalent interactions is the concurrent existence of a complex ring system (including neutral [π]

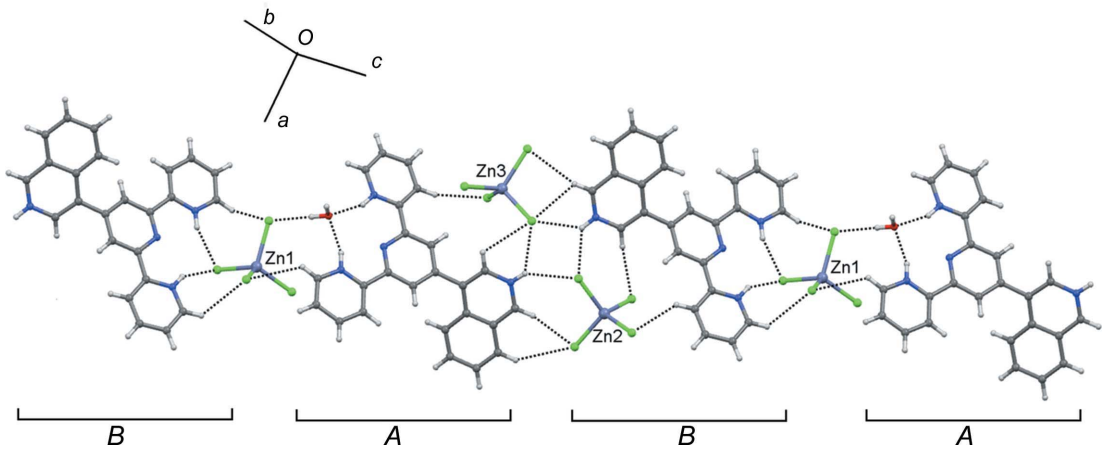

Figure 3
A combined version of Figs. 2(*c*) and 2(*d*), showing the collective bridging action of all three tcz cations in the [11$\bar{1}$] direction.

or charged [π^+] ones) and a diversity of Cl^- anions giving rise to a number of so-called anion$\cdots\pi$ interactions. Even after having been detected and described for years, it is only recently that these anion$\cdots\pi$ contacts have been given full credit as relevant noncovalent interactions, and have accordingly received due theoretical attention (Giese *et al.*, 2015; Gamez, 2014; Bauza *et al.*, 2016). Their systematic study led to the development of a number of 'working rules' which enabled the analysis of any particular geometrical anion$\cdots\pi$ disposition, permitting its acceptance (or rejection) as a feasible

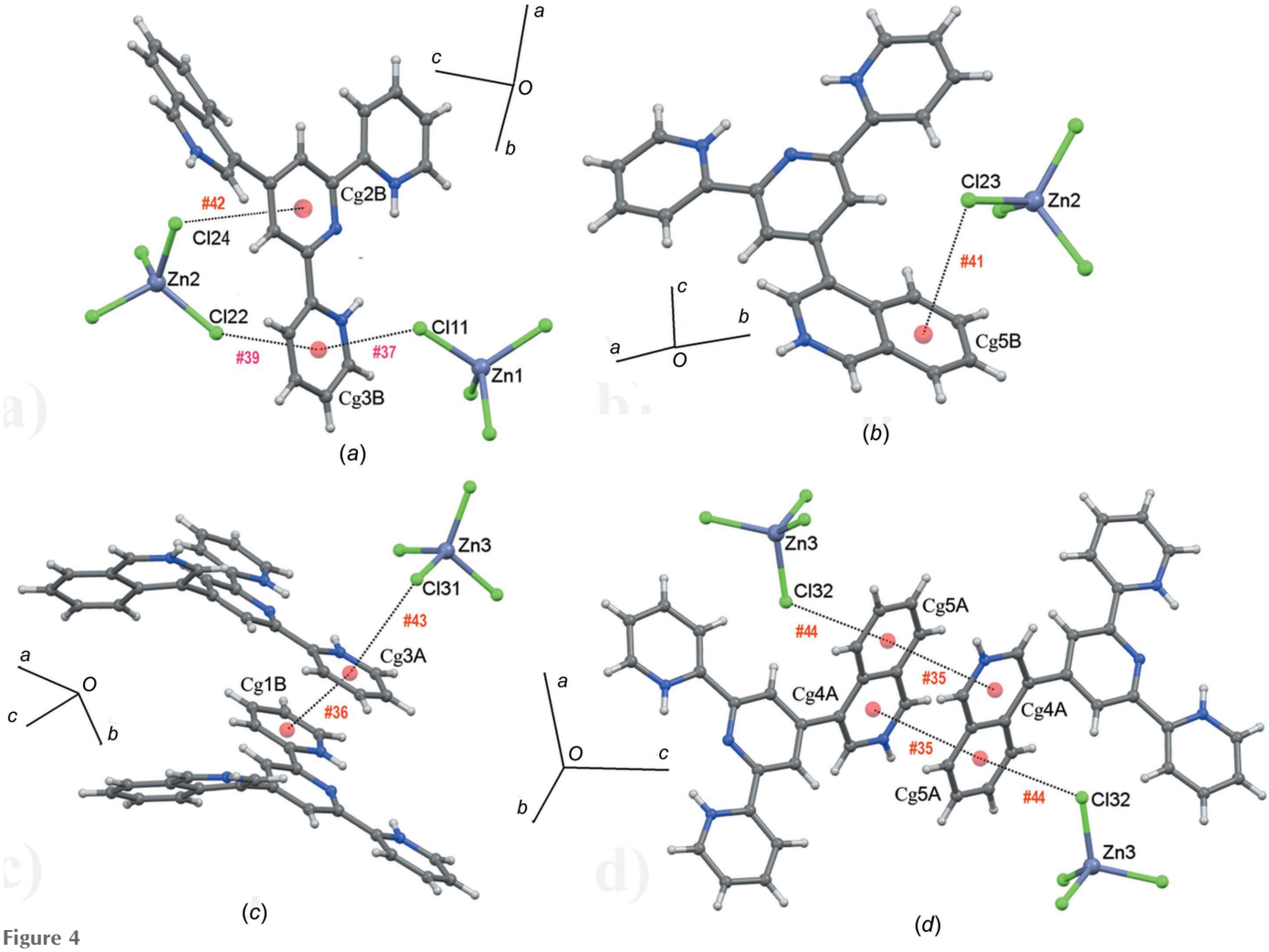

Figure 4
(*a*)/(*b*) Anion$\cdots\pi$ interactions in (**II**), with no π-stacking. (*c*)/(*d*) Anion$\cdots\pi$–π interactions.

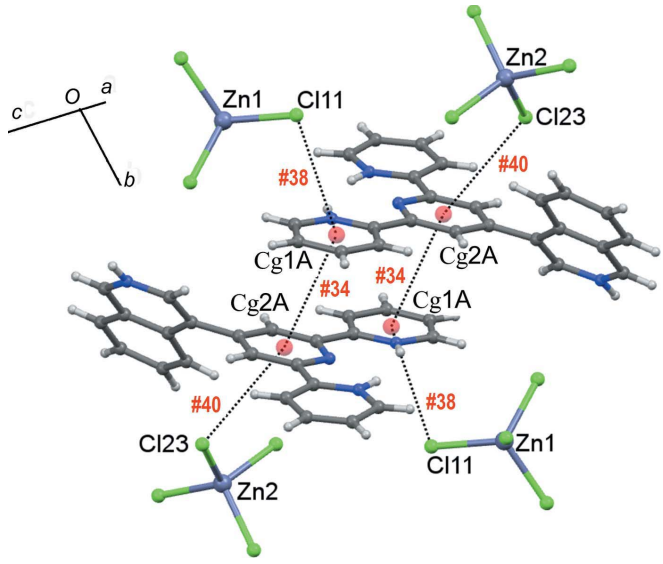

Figure 5
Anion···π–π···anion interactions in (**II**).

interaction worthy of analysis. In Table 5 and the supporting information (§SI4), we present these rules, as well as the interactions in (**II**) which have passed this 'geometrical screening'. In particular, a confirmation of the relevance of these anion···π interactions can be grasped from a search in the CSD, which afforded about 80000 similar Cl···π interactions (as defined by the CSD default values), showing a population maximum (or mode) of the X—Cl···C distance at ∼3.62 Å, while the mean value in the present structure is 3.41 (14) Å. Figs. 4 and 5 present a detailed description of the way in which the tcz anions are connected with the $(ITPH_3)^{3+}$ cations through these interactions, either on their own (as simple anion···π interactions; Figs. 4*a* and 4*b*) or in conjunction with π-stacking in what could be called 'combined anion···π–π interactions' (Figs. 4*c* and 4*d*) or more complex still, 'anion···π–π···anion' interactions (Fig. 5). All three π-stacking interactions presented in Table 4 appear in these combined forms. At first glance, the different types of $[XCl_4]^{2-}$ anions (X = Fe, Co, Ni, Cu, Zn, Ga, *etc.*) appear to be well suited for this type of interaction. The CSD was searched and the results are summarized in Fig. 6, sorted according to the increasing complexity of the interactions, in the same way as those appearing in Figs. 4 and 5. It is apparent that the frequency with which each type is found (Fig. 6 caption) decreases with increasing complexity, and, in particular, pairwise interactions involving covalently bonded rings are significantly rarer (Fig. 6, bottom). For the case where there is one single anion on each side of the centrosymmetric array (d_1), there are three cases reported in the CSD (see Fig. 6 for details); for the remaining one, instead, with two independent anions at each side, *i.e.* (d_2), there are no examples in the CSD, the present structure (**II**) being the first to be reported.

Up to this stage, we had fully characterized and analyzed in detail each interaction in the complete #1 to #43 set, with due assessment of their absolute and relative importance on individual terms. But even so, there are no clear clues as to which type of interaction (if any at all) is mainly responsible for the crystal stability, much in the same way as individual trees may eventually hide the forest. An alternative, global

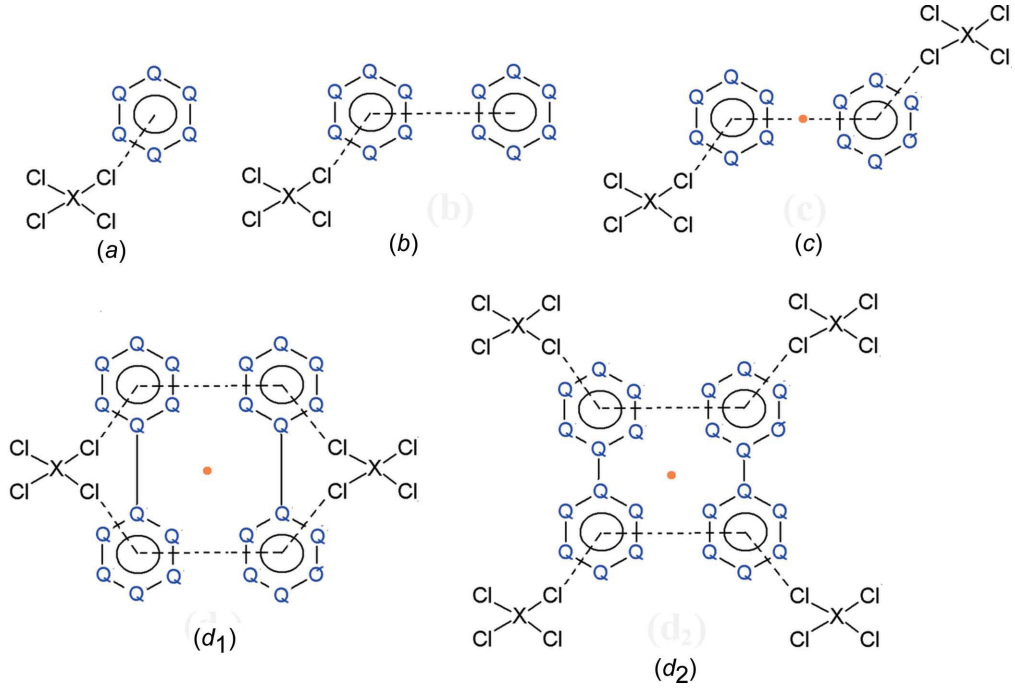

Figure 6
The frequency with which different types of anion···π patterns appear in the literature. (*a*) 904 cases, (*b*) 199 cases, (*c*) 24 cases, (d_1) 3 cases [CSD refcodes AWEJUH and PINNUV01 (Zhang *et al.*, 2003) and GEPYIJ10 (Constable *et al.*, 1991)] and (d_2) 1 case [structure (**II**), this work]. Orange circles represent inversion centres.

analysis was thus needed and we found in ER (presented in §2.3) an adequate approach which produced some unexpected results.

3.2. Hirshfeld surface and enrichment ratio (ER) analysis

3.2.1. The global contacts. The computed Hirshfeld surfaces and the corresponding enrichment ratios of the contacts in the global structure are shown in Table 6, where the H atoms bound to carbon (H_C), nitrogen (H_N) and oxygen (H_{OH}) are differentiated. As expected, the most important contributions to the global surface (taking into account the inner and outer surfaces) are provided by the C (26.15%), Cl (33.48%) and H_C (27.00%) species. In addition, there are some further favoured enrichment ratios which appear reasonable, *viz*. those involving the chloride anions [$H_{OH}\cdots$Cl (1.99), $H_C\cdots$Cl (1.92) and $H_N\cdots$Cl (1.73)] and the O atom of the water molecule ($H_N\cdots$O 18.19). For the special case of the enriched $H_C\cdots$Zn interaction (2.48), it has been suggested that this results from the closeness of the relevant $H_C\cdots$Cl interactions (El Glaoui *et al.*, 2017). A surprising fact, however, was to find an increase in the enrichment ratio of contacts between atoms of the $(ITPH_3)^{3+}$ cations [C$\cdots$C (1.47) and C$\cdots$N (2.25); Table 6], compared with those of neutral free (**I**) [C$\cdots$C (1.17) and C$\cdots$N (0.92); Table 7], despite the former having an *ab initio* drawback, *viz*. the electrostatic repulsion between charges of same the sign.

3.2.2. The cationic contacts. In an attempt to highlight the reasons for this unexpected enrichment of the C$\cdots$C and C$\cdots$N contacts involving the $(ITPH_3)^{3+}$ cations, we separately evaluated the Hirshfeld surfaces of the two organic cations

Table 6
Hirshfeld contact surfaces and enrichment ratios (ERs) for $(ITPH_3)_2[ZnCl_4]_3{\cdot}H_2O$, computed around the two $(ITPH_3)^{3+}$ cations (*A* and *B*), the three $[ZnCl_4]^{2-}$ anions and the water molecule.

The first column corresponds to 'interior' atoms; the remaining columns to 'exterior' ones. The reported values correspond to the (merged) reciprocal contacts.

	C	N	O	Cl	Zn	H_C	H_N	H_{OH}
Actual contacts (merged) (%)								
C	10.01							
N	2.94	0.00						
O	0.16	0.02	0.00					
Cl	18.62	1.44	0.00	2.02				
Zn	1.54	0.00	0.00	0.31	0.00			
H_C	7.74	0.62	0.25	34.66	4.49	2.40		
H_N	0.92	0.00	1.62	5.03	0.15	0.76	0.00	
H_{OH}	0.35	0.00	0.00	2.86	0.20	0.67	0.21	0.00
Surface interior (%)	27.32	2.71	0.99	32.20	3.19	27.18	4.30	2.10
Surface exterior (%)	24.98	2.30	1.05	34.76	3.51	26.81	4.38	2.20
Enrichment ratios (merged)								
C	1.47							
N	2.25	0.00						
O	0.30	0.45	0.00					
Cl	1.06	0.85	0.00	0.18				
Zn	0.88	0.00	0.00	0.14	0.00			
H_C	0.55	0.46	0.45	1.92	2.48	0.33		
H_N	0.41	0.00	18.19	1.73	0.50	0.32	0.00	
H_{OH}	0.31	0.00	0.00	1.99	1.42	0.58	1.14	0.00

Table 7
Hirshfeld contact surfaces and enrichment ratios for ITP.

The first column corresponds to 'interior' atoms; the remaining columns to 'exterior' ones. The reported values correspond to the (merged) reciprocal contacts.

	C	N	H_C
Actual contacts (merged) (%)			
C	21.45		
N	7.05	0.25	
H_C	35.69	10.40	25.16
Surface interior (%)	44.42	9.11	46.47
Surface exterior (%)	41.22	8.84	49.94
Enrichment ratios (merged)			
C	1.17		
N	0.92	0.31	
H_C	0.86	1.20	1.08

(Figs. 7 and 8). Tables SI5a and SI5b (see supporting information) show the surface composition of $(ITPH_3)^{3+}$ cations *A* and *B*, respectively. Both structures present a very similar distribution of the Hirshfeld surface (adding the inner and outer surfaces), where the C, Cl and H_C species are the most relevant (*A*: 35.34, 23.58 and 27.90%; *B*: 32.64, 25.76 and 30.54%, respectively). The similarities are also present when the values of the enrichment ratios (due only to intermolecular interactions between the organic fragments) are compared (Tables SI5a and SI5b in the supporting information). Thus, in both cations, the magnitude of the most strongly enriched contacts, *i.e.* C$\cdots$C (*A* 1.54 and *B* 1.35) and C$\cdots$N (*A* 2.19 and *B* 1.88), are comparable, those in cation *A* being only slightly larger than those in cation *B* and with C$\cdots$N interactions being the most favoured. With these precedents, a puzzling situation appears when π–π interactions are considered (Table 4), in which all five rings in cation *A* participate, while this is true of only a single ring of cation *B* (*Cg*1*B*). This should, in principle, be reflected in a pronounced difference in the ER values for the C$\cdots$C and C$\cdots$N contacts (*A* > *B*), something which is far from what is observed. On the other hand, an even more different situation exists when the number of anion$\cdots\pi$ interactions are compared; there are four on the surface of cation *A* and four on the surface of cation *B* (Table 5). This is consistent with the driving force for the crystal packing of (**II**) being strongly influenced by anion$\cdots\pi$ interactions, where the Cl^- anions are attracted by the cationic aromatic rings reducing the strong cationic charge–charge repulsion and in some way favouring the C$\cdots$C and mainly the C$\cdots$ N contacts, which denotes a reorientation of the π–π interactions with respect to the situation in the unprotonated moieties.

These observations indicated a preferred orientation of the cationic π–π contacts that could be explained by visualizing the distribution of the positive charge on protonation. In this regard, the atomic and ring NBO (natural bond order) charges for a series of aromatic N-heterocyclic compounds, both neutral and protonated, have been calculated recently by Maclagan and co-workers (Maclagan *et al.*, 2015). Remarkably, it was concluded that in all protonated ions both the

N—H hydrogen and the N—H nitrogen carry almost a constant charge 'q', with an average of q(H) = 0.43 ± 0.01 and q(N) = −0.46 ± 0.1. Furthermore, the remaining positive charge, *i.e.* 0.57 ± 0.01 unit charge from the full proton, is dispersed over the rest of the aromatic rings, *i.e.* over the C and H atoms. Another surprising result is that the N atom maintains almost without change its preponderance as the higher negative charge when passing from the neutral species to the ionic one. In fact, the q(N) values of the neutral base are not significantly different from those when it is protonated, *e.g.* in the pyridine(−0.45)/pyridineH^+(−0.44) and quinoline/(−0.45)/quinolineH^+(−0.44) pairs. These results permit us to attribute the great enrichment of the cationic C···N interactions to the increase in the positive charge on the C atoms and to the almost unchanged negative charge on the N atoms. On the other hand, the fact that the positive charge (0.57 ± 0.01 unit charge) is dispersed towards the C and H atoms of the aromatic hydrocarbon rings explains the abundance, firstly, of the anion···π interactions and, secondly, of those around the periphery of the planes of the aromatic rings, namely the H_C···Cl interactions.

3.2.3. The anionic contacts (Hirshfeld surfaces and AIM analysis). The percent contributions to the Hirshfeld surface of the $[ZnCl_4]^{2-}$···X contacts involving the three anions (taken individually) are shown in Table 8. The two most important contributions that are observed in the exterior surfaces come from weak $[ZnCl_4]^{2-}$···H_C interactions, with an average of 52.81%, and the other most frequent contacts are the impor-

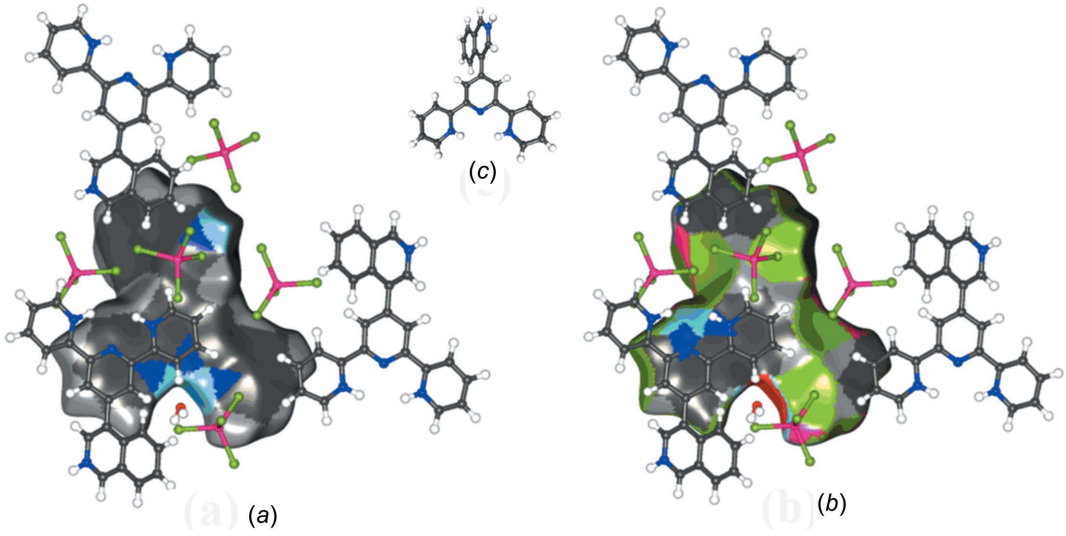

Figure 7
Hirshfeld surface of $(ITPH_3)^{3+}$ cation *A* and the most relevant species on the surface, showing (*a*) the surface coloured according to the interior atoms, (*b*) the surface coloured according to the exterior atoms and (*c*) the orientation of the structure inside the surface. Colour key: HC grey, HN/O light blue, C dark brown, N blue, Cl^- green, O red and Zn purple.

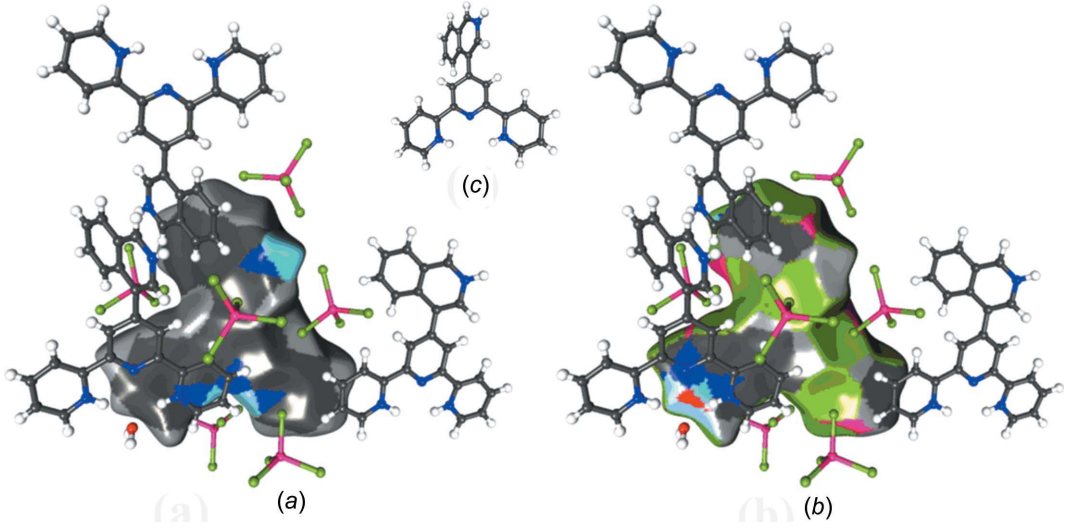

Figure 8
Hirshfeld surface of $(ITPH_3)^{3+}$ cation *B* and the most relevant species on the surface, showing (*a*) the surface coloured according to the interior atoms, (*b*) the surface coloured according to the exterior atoms and (*c*) the orientation of the structure inside the surface. Colour key: HC grey, HN/O light blue, C dark brown, N blue, Cl^- green, O red and Zn purple.

tant $[ZnCl_4]^{2-}\cdots C$ interactions, with an average of 26.87%. Furthermore, Tables 3–5 show that Cl$\cdots X$ interactions (as evaluated by AIM) are relevant when compared to the remaining interactions in the system. With typical values of ∼1.00 a.u., even if they are ranked second to N—H$\cdots$O (∼2.5 a.u.), they appear to be of similar strength to many C—H$\cdots$Cl interactions and significantly stronger than π–π interactions (∼0.5 a.u.). Thus, the Cl$\cdots X$ interactions show an individual relevance, which, in addition to the large number of these contacts, enhance their importance in crystal structure stabilization.

4. Conclusions

The structural study of the new protonated terpyridine-based compound, $(ITPH_3)_2[ZnCl_4]_3{\cdot}H_2O$, (**II**), presenting five independent ionic entities, *i.e.* two $(ITPH_3)^{3+}$ cations and three $[ZnCl_4]^{2-}$ anions, demonstrates the concerted way in which a variety of noncovalent interactions, *viz.* hydrogen bonding, anion$\cdots\pi$ and π–π stacking, participate in the crystal packing. The repulsive nature of the π–π stacking between the triply protonated $(ITPH_3)^{3+}$ cations is counteracted by the $[ZnCl_4]^{2-}$ anions through abundant peripheral hydrogen bonding and anion$\cdots\pi$ interactions involving the ring planes. These latter interactions are involved in several types of arrangements, either without π-stacking (as simple anion$\cdots\pi$) or more complex ones with π–π stacking in the acceptors (as anion$\cdots\pi$–π and the rare case of anion$\cdots\pi$–$\pi\cdots$anion).

From a theoretical point of view, the unexpectedly large enrichment ratios (ER) of the cationic C$\cdots$N contacts observed in (**II**) can be understood in the light of their correlation with the atomic and ring NBO charges. On the other hand, with regard to the significance of the not-so-frequent Cl$\cdots\pi$ interactions in the structure stabilization, AIM results tell us that even if they rank second with respect to N—H$\cdots$O interactions, they are comparable to many C—H$\cdots$Cl interactions in the structure and significantly stronger than π–π interactions.

Funding information

Funding for this research was provided by: NPCyT (project No. PME 2006-01113, for the purchase of the Oxford Gemini CCD diffractometer); Universidad de La Frontera (project No. DIUFRO DI17-0173).

Table 8
Hirshfeld contact surfaces (%) for the $[ZnCl_4]^{2-}\cdots X$ contacts.

Surface	C	N	O	Cl	Zn	H_C	H_N	H_{OH}
Zn1 interior	0.00	0.00	0.00	90.99	9.01	0.00	0.00	0.00
Zn1 exterior	20.61	3.11	0.00	8.13	1.37	51.37	9.80	5.61
Zn2 interior	0.00	0.00	0.00	91.34	8.66	0.00	0.00	0.00
Zn2 exterior	37.11	0.79	0.00	4.81	0.00	51.61	5.68	0.00
Zn3 interior	0.00	0.00	0.00	89.97	10.03	0.00	0.00	0.00
Zn3 exterior	22.90	1.14	0.00	6.93	0.00	55.46	6.32	7.26

References

Bader, R. F. W. (1990). In *In Atoms in Molecules – a Quantum Theory*. Oxford University Press.
Bader, R. F. W. (2009). *J. Phys. Chem. A*, **113**, 10391–10396.
Bauza, A., Mooibroek, T. J. & Frontera, A. (2016). *CrystEngComm*, **18**, 10–23.
Bruno, I. J., Cole, J. C., Edgington, P. R., Kessler, M., Macrae, C. F., McCabe, P., Pearson, J. & Taylor, R. (2002). *Acta Cryst.* B**58**, 389–397.
Chen, Ch., Jin, X.-H., Zhou, X.-J., Cai, L.-X., Zhang, Y.-J. & Zhang, J. (2015). *J. Mater. Chem. C*, **3**, 4563–4569.
Constable, E. C., Khan, M. S., Lewis, J., Liptrot, M. C. & Raithby, P. R. (1991). *Inorg. Chim. Acta*, **187**, 1–4.
El Glaoui, M., El Glaoui, M., Jelsch, C., Aubert, E., Lefebvre, F. & Ben Nasr, C. (2017). *J. Mol. Struct.* **1134**, 538–545.
Frisch, M. J., *et al.* (2009). *GAUSSIAN03*. Gaussian Inc., Wallingford, Connecticut, USA.
Gamez, P. (2014). *Inorg. Chem. Front.* **1**, 35–43.
Giese, M., Albrecht, M. & Rissanen, K. (2015). *Chem. Rev.* **115**, 8867–8895.
Granifo, J., Arévalo, B., Gaviño, R., Suárez, S. & Baggio, R. (2016). *Acta Cryst.* C**72**, 932–938.
Grimme, S., Antony, J., Ehrlich, S. & Krieg, S. (2010). *J. Chem. Phys.* **132**, 154104.
Groom, C. R., Bruno, I. J., Lightfoot, M. P. & Ward, S. C. (2016). *Acta Cryst.* B**72**, 171–179.
Guillot, B. (2011). *Acta Cryst.* A**67**, C511–C512.
Hay, P. J. & Wadt, W. R. (1985). *J. Chem. Phys.* **82**, 270-283
Janiak, C. (2000). *J. Chem. Soc. Dalton Trans.* pp. 3885–3898.
Jelsch, C., Ejsmont, K. & Huder, L. (2014). *IUCrJ*, **1**, 119–128.
Lu, T. & Chen, F. (2012). *J. Comput. Chem.* **33**, 580–592.
Maclagan, R. G. A. R., Gronert, S. & Meot-Ner, M. (2015). *J. Phys. Chem. A*, **119**, 127–139.
Manna, P., Seth, S. K., Bauza, A., Mitra, M., Choudhury, S. R., Frontera, A. & Mukhopadhyay, S. (2014*a*). *Cryst. Growth Des.* **14**, 747–755.
Manna, P., Seth, S. K., Mitra, M., Choudhury, S. R., Bauza, A., Frontera, A. & Mukhopadhyay, S. (2014*b*). *Cryst. Growth Des.* **14**, 5812–5821.
Manna, P., Seth, S. K., Mitra, M., Das, A., Singh, N. J., Choudhury, S. R., Kar, T. & Mukhopadhyay, S. (2013). *CrystEngComm*, **15**, 7879–7886.
Padhi, S. K., Sahu, R., Saha, D. & Manivannan, V. (2011). *Inorg. Chim. Acta*, **372**, 383–388.
Perdew, J. P., Burke, K. & Ernzerhof, M. (1996). *Phys. Rev. Lett.* **77**, 3865–3868.
Perdew, J. P., Burke, K. & Ernzerhof, M. (1997). *Phys. Rev. Lett.* **78**, 1396.
Rigaku Oxford Diffraction (2015). *CrysAlis PRO*. Rigaku Oxford Diffraction Ltd, Yarnton, Oxfordshire, England.
Seth, S. K., Manna, P., Singh, N. J., Mitra, M., Jana, A. D., Das, A., Choudhury, S. R., Kar, T., Mukhopadhyay, S. & Kim, K. S. (2013). *CrystEngComm*, **15**, 1285–1288.
Sheldrick, G. M. (2008). *Acta Cryst.* A**64**, 112–122.
Sheldrick, G. M. (2015). *Acta Cryst.* C**71**, 3–8.
Spackman, M. A. & Byrom, P. G. (1997). *Chem. Phys. Lett.* **267**, 215–220.
Spek, A. L. (2009). *Acta Cryst.* D**65**, 148–155.
Yang, Y., Weaver, M. N. & Merz, K. M. (2009). *J. Phys. Chem. A*, **113**, 9843–9851.
Yarwood, J., Douthwaite, R. & Duckett, S. (2009). Editors. *Spectroscopic Properties of Inorganic and Organometallic Compounds*, Vol. 40, pp. 200–201. London: Royal Society of Chemistry.
Zhang, R.-L., Liu, H.-M., Zhao, J.-S., Gu, A.-P., He, S.-Y., Liu, J.-N. & Shi, Q.-Z. (2003). *Chin. J. Inorg. Chem.* **19**, 722–726.

supporting information

Acta Cryst. (2017). C**73**, 1121-1130 [https://doi.org/10.1107/S2053229617016308]

Crystallographic and computational study of a network composed of $[ZnCl_4]^{2-}$ anions and triply protonated 4′-functionalized terpyridine cations

Juan Granifo, Sebastián Suárez, Fernando Boubeta and Ricardo Baggio

Computing details

Data collection: *CrysAlis PRO* (Rigaku Oxford Diffraction, 2015); cell refinement: *CrysAlis PRO* (Rigaku Oxford Diffraction, 2015); data reduction: *CrysAlis PRO* (Rigaku Oxford Diffraction, 2015); program(s) used to solve structure: *SHELXS97* (Sheldrick, 2008); program(s) used to refine structure: *SHELXL2014* (Sheldrick, 2015); molecular graphics: *SHELXTL* (Sheldrick, 2008) and *Mercury* (Bruno *et al.*, 2002); software used to prepare material for publication: *SHELXL2014* (Sheldrick, 2015) and *PLATON* (Spek, 2009).

Bis[4′-(isoquinolin-2-ium-4-yl)-2,2′:6′,2′-terpyridine-1,1′′-diium] tris[tetrachloridozincate(II)] monohydrate

Crystal data

$(C_{24}H_{19}N_4)_2[ZnCl_4]_3\cdot H_2O$
M_r = 1366.39
Triclinic, $P\overline{1}$
a = 11.0485 (6) Å
b = 16.0249 (8) Å
c = 16.4318 (7) Å
α = 100.824 (4)°
β = 103.574 (4)°
γ = 102.737 (4)°
V = 2668.9 (2) Å^3
Z = 2
$F(000)$ = 1372
D_x = 1.700 Mg m^{-3}
Mo $K\alpha$ radiation, λ = 0.71073 Å
Cell parameters from 4044 reflections
θ = 3.5–28.4°
μ = 1.98 mm^{-1}
T = 150 K
Prism, colourless
0.30 × 0.25 × 0.20 mm

Data collection

Rigaku Xcalibur Sapphire3 diffractometer
Radiation source: fine-focus sealed X-ray tube, Enhance (Mo) X-ray Source
Graphite monochromator
ω scans
Absorption correction: multi-scan CrysAlisPro 1.171.38.41r (Rigaku Oxford Diffraction, 2015)
T_{min} = 0.54, T_{max} = 0.70
29335 measured reflections
12387 independent reflections
9230 reflections with $I > 2\sigma(I)$
R_{int} = 0.049
θ_{max} = 28.9°, θ_{min} = 3.3°
h = −14→13
k = −21→20
l = −22→22

Refinement

Refinement on F^2
Least-squares matrix: full
$R[F^2 > 2\sigma(F^2)]$ = 0.043
$wR(F^2)$ = 0.092
S = 0.93
12387 reflections
673 parameters
9 restraints
Hydrogen site location: mixed
H atoms treated by a mixture of independent and constrained refinement

$w = 1/[\sigma^2(F_o^2) + (0.0298P)^2 + 4.101P]$
where $P = (F_o^2 + 2F_c^2)/3$
$(\Delta/\sigma)_{max} = 0.001$

$\Delta\rho_{max} = 0.66$ e Å^{-3}
$\Delta\rho_{min} = -0.48$ e Å^{-3}

Special details

Geometry. All e.s.d.'s (except the e.s.d. in the dihedral angle between two l.s. planes) are estimated using the full covariance matrix. The cell e.s.d.'s are taken into account individually in the estimation of e.s.d.'s in distances, angles and torsion angles; correlations between e.s.d.'s in cell parameters are only used when they are defined by crystal symmetry. An approximate (isotropic) treatment of cell e.s.d.'s is used for estimating e.s.d.'s involving l.s. planes.

Fractional atomic coordinates and isotropic or equivalent isotropic displacement parameters (Å^2)

	x	*y*	*z*	U_{iso}*/U_{eq}
Zn1	0.74573 (4)	0.87831 (3)	0.94630 (2)	0.01807 (10)
Cl11	0.79844 (8)	0.84870 (5)	1.07678 (5)	0.01833 (17)
Cl12	0.85218 (8)	1.01854 (5)	0.94663 (5)	0.01772 (17)
Cl13	0.52863 (8)	0.87294 (6)	0.90934 (5)	0.02331 (19)
Cl14	0.78516 (10)	0.78122 (6)	0.84490 (6)	0.0287 (2)
Zn2	0.28439 (4)	0.19736 (2)	0.56472 (2)	0.01446 (9)
Cl21	0.19816 (8)	0.24136 (5)	0.67270 (5)	0.01877 (18)
Cl22	0.17120 (8)	0.20948 (6)	0.43425 (5)	0.01898 (18)
Cl23	0.49308 (8)	0.28265 (5)	0.59620 (5)	0.01552 (17)
Cl24	0.28899 (8)	0.05541 (5)	0.55881 (5)	0.01903 (18)
Zn3	−0.04607 (4)	0.44630 (3)	0.25013 (2)	0.01746 (10)
Cl31	−0.00734 (9)	0.44474 (6)	0.12015 (5)	0.02125 (18)
Cl32	−0.26513 (8)	0.40361 (6)	0.23286 (5)	0.01881 (18)
Cl33	0.02092 (9)	0.33585 (6)	0.30103 (6)	0.0259 (2)
Cl34	0.05301 (9)	0.58200 (6)	0.33859 (5)	0.0258 (2)
N1A	0.4258 (3)	0.36566 (18)	0.98779 (17)	0.0160 (6)
H1NA	0.492 (2)	0.346 (2)	0.996 (2)	0.019*
N2A	0.5850 (3)	0.37384 (17)	0.88918 (17)	0.0147 (6)
N3A	0.7740 (3)	0.30000 (18)	0.93739 (18)	0.0169 (6)
H3NA	0.719 (3)	0.306 (2)	0.965 (2)	0.020*
N4A	0.6751 (3)	0.63017 (18)	0.64108 (18)	0.0173 (6)
H4NA	0.743 (2)	0.6668 (18)	0.641 (2)	0.021*
C1A	0.3542 (3)	0.3561 (2)	1.0424 (2)	0.0176 (7)
H1A	0.3761	0.3270	1.0852	0.021*
C2A	0.2488 (3)	0.3889 (2)	1.0359 (2)	0.0192 (7)
H2A	0.1982	0.3822	1.0734	0.023*
C3A	0.2198 (3)	0.4327 (2)	0.9712 (2)	0.0200 (7)
H3A	0.1499	0.4568	0.9659	0.024*
C4A	0.2948 (3)	0.4405 (2)	0.9148 (2)	0.0173 (7)
H4A	0.2743	0.4688	0.8711	0.021*
C5A	0.3999 (3)	0.4064 (2)	0.9234 (2)	0.0135 (7)
C6A	0.4916 (3)	0.4129 (2)	0.8702 (2)	0.0141 (7)
C7A	0.4803 (3)	0.4589 (2)	0.8062 (2)	0.0145 (7)
H7A	0.4131	0.4850	0.7945	0.017*
C8A	0.5708 (3)	0.4653 (2)	0.76012 (19)	0.0137 (7)
C9A	0.6699 (3)	0.4252 (2)	0.78013 (19)	0.0144 (7)

H9A	0.7325	0.4284	0.7508	0.017*
C10A	0.6733 (3)	0.3801 (2)	0.8450 (2)	0.0152 (7)
C11A	0.7741 (3)	0.3348 (2)	0.8686 (2)	0.0150 (7)
C12A	0.8665 (3)	0.3246 (2)	0.8263 (2)	0.0185 (7)
H12A	0.8705	0.3486	0.7793	0.022*
C13A	0.9534 (3)	0.2780 (2)	0.8550 (2)	0.0231 (8)
H13A	1.0149	0.2699	0.8264	0.028*
C14A	0.9491 (3)	0.2439 (2)	0.9252 (2)	0.0243 (8)
H14A	1.0068	0.2125	0.9442	0.029*
C15A	0.8587 (3)	0.2568 (2)	0.9667 (2)	0.0218 (8)
H15A	0.8560	0.2355	1.0153	0.026*
C16A	0.5655 (3)	0.5178 (2)	0.6940 (2)	0.0142 (7)
C17A	0.6759 (3)	0.5770 (2)	0.6971 (2)	0.0162 (7)
H17A	0.7530	0.5815	0.7378	0.019*
C18A	0.5681 (3)	0.6284 (2)	0.5834 (2)	0.0188 (7)
H18A	0.5712	0.6671	0.5478	0.023*
C19A	0.4502 (3)	0.5686 (2)	0.5757 (2)	0.0159 (7)
C20A	0.3357 (3)	0.5666 (2)	0.5144 (2)	0.0206 (8)
H20A	0.3377	0.6059	0.4794	0.025*
C21A	0.2218 (4)	0.5067 (2)	0.5066 (2)	0.0226 (8)
H21A	0.1457	0.5060	0.4671	0.027*
C22A	0.2196 (3)	0.4459 (2)	0.5583 (2)	0.0191 (7)
H22A	0.1420	0.4045	0.5517	0.023*
C23A	0.3293 (3)	0.4465 (2)	0.6180 (2)	0.0160 (7)
H23A	0.3261	0.4050	0.6506	0.019*
C24A	0.4473 (3)	0.5097 (2)	0.63051 (19)	0.0134 (7)
N1B	0.6444 (3)	0.07957 (18)	0.83412 (17)	0.0150 (6)
H1NB	0.706 (2)	0.056 (2)	0.845 (2)	0.018*
N2B	0.8062 (3)	0.06720 (17)	0.73738 (16)	0.0141 (6)
N3B	0.9733 (3)	−0.02531 (19)	0.78502 (18)	0.0177 (6)
H3NB	0.919 (3)	−0.015 (2)	0.811 (2)	0.021*
N4B	0.8957 (3)	0.25376 (19)	0.43406 (18)	0.0169 (6)
H4NB	0.9668 (19)	0.276 (2)	0.425 (2)	0.020*
C1B	0.5685 (3)	0.0794 (2)	0.8869 (2)	0.0171 (7)
H1B	0.5861	0.0558	0.9345	0.021*
C2B	0.4653 (3)	0.1139 (2)	0.8707 (2)	0.0195 (7)
H2B	0.4110	0.1127	0.9062	0.023*
C3B	0.4431 (3)	0.1505 (2)	0.8011 (2)	0.0183 (7)
H3B	0.3736	0.1746	0.7895	0.022*
C4B	0.5245 (3)	0.1513 (2)	0.7480 (2)	0.0164 (7)
H4B	0.5101	0.1765	0.7013	0.020*
C5B	0.6268 (3)	0.1145 (2)	0.76484 (19)	0.0141 (7)
C6B	0.7188 (3)	0.1097 (2)	0.71316 (19)	0.0132 (7)
C7B	0.7108 (3)	0.1476 (2)	0.6429 (2)	0.0139 (7)
H7B	0.6504	0.1789	0.6297	0.017*
C8B	0.7948 (3)	0.1378 (2)	0.5929 (2)	0.0138 (7)
C9B	0.8877 (3)	0.0947 (2)	0.6187 (2)	0.0154 (7)
H9B	0.9468	0.0881	0.5876	0.018*

C10B	0.8919 (3)	0.0613 (2)	0.6918 (2)	0.0135 (7)
C11B	0.9874 (3)	0.0131 (2)	0.7199 (2)	0.0140 (7)
C12B	1.0883 (3)	0.0055 (2)	0.6864 (2)	0.0174 (7)
H12B	1.1017	0.0325	0.6426	0.021*
C13B	1.1702 (3)	−0.0425 (2)	0.7182 (2)	0.0203 (8)
H13B	1.2380	−0.0484	0.6951	0.024*
C14B	1.1517 (4)	−0.0818 (2)	0.7839 (2)	0.0244 (8)
H14B	1.2062	−0.1143	0.8053	0.029*
C15B	1.0514 (3)	−0.0720 (2)	0.8171 (2)	0.0229 (8)
H15B	1.0375	−0.0976	0.8616	0.028*
C16B	0.7860 (3)	0.1736 (2)	0.5153 (2)	0.0133 (7)
C17B	0.8985 (3)	0.2176 (2)	0.5026 (2)	0.0163 (7)
H17B	0.9776	0.2227	0.5414	0.020*
C18B	0.7858 (3)	0.2519 (2)	0.3786 (2)	0.0182 (7)
H18B	0.7882	0.2809	0.3348	0.022*
C19B	0.6669 (3)	0.2071 (2)	0.3855 (2)	0.0147 (7)
C20B	0.5502 (3)	0.2018 (2)	0.3239 (2)	0.0190 (7)
H20B	0.5523	0.2306	0.2799	0.023*
C21B	0.4348 (3)	0.1546 (2)	0.3291 (2)	0.0201 (8)
H21B	0.3579	0.1520	0.2893	0.024*
C22B	0.4322 (3)	0.1101 (2)	0.3946 (2)	0.0189 (7)
H22B	0.3530	0.0775	0.3973	0.023*
C23B	0.5437 (3)	0.1133 (2)	0.4549 (2)	0.0152 (7)
H23B	0.5393	0.0820	0.4969	0.018*
C24B	0.6651 (3)	0.1637 (2)	0.45367 (19)	0.0123 (6)
O1W	0.6211 (2)	0.29045 (16)	1.04752 (15)	0.0204 (5)
H1WA	0.668 (3)	0.3251 (18)	1.0996 (11)	0.031*
H1WB	0.579 (3)	0.2402 (13)	1.057 (2)	0.031*

Atomic displacement parameters (Å²)

	U^{11}	U^{22}	U^{33}	U^{12}	U^{13}	U^{23}
Zn1	0.0231 (2)	0.0182 (2)	0.0170 (2)	0.00700 (17)	0.00999 (17)	0.00704 (16)
Cl11	0.0191 (4)	0.0225 (4)	0.0185 (4)	0.0096 (3)	0.0083 (3)	0.0091 (3)
Cl12	0.0170 (4)	0.0205 (4)	0.0189 (4)	0.0065 (3)	0.0055 (3)	0.0107 (3)
Cl13	0.0203 (5)	0.0270 (5)	0.0210 (4)	0.0024 (4)	0.0039 (3)	0.0097 (4)
Cl14	0.0468 (6)	0.0231 (5)	0.0232 (5)	0.0114 (4)	0.0210 (4)	0.0065 (4)
Zn2	0.0143 (2)	0.01442 (19)	0.01503 (19)	0.00396 (16)	0.00357 (15)	0.00529 (15)
Cl21	0.0193 (4)	0.0208 (4)	0.0195 (4)	0.0071 (3)	0.0087 (3)	0.0071 (3)
Cl22	0.0155 (4)	0.0244 (4)	0.0178 (4)	0.0057 (3)	0.0031 (3)	0.0090 (3)
Cl23	0.0146 (4)	0.0148 (4)	0.0168 (4)	0.0034 (3)	0.0032 (3)	0.0059 (3)
Cl24	0.0249 (5)	0.0134 (4)	0.0207 (4)	0.0052 (3)	0.0096 (3)	0.0053 (3)
Zn3	0.0154 (2)	0.0216 (2)	0.0173 (2)	0.00586 (17)	0.00472 (16)	0.00865 (17)
Cl31	0.0248 (5)	0.0227 (4)	0.0178 (4)	0.0059 (4)	0.0090 (3)	0.0060 (3)
Cl32	0.0161 (4)	0.0232 (4)	0.0187 (4)	0.0084 (3)	0.0049 (3)	0.0055 (3)
Cl33	0.0179 (5)	0.0341 (5)	0.0375 (5)	0.0120 (4)	0.0125 (4)	0.0256 (4)
Cl34	0.0297 (5)	0.0252 (5)	0.0189 (4)	0.0021 (4)	0.0060 (4)	0.0048 (4)
N1A	0.0152 (15)	0.0159 (14)	0.0166 (14)	0.0028 (12)	0.0056 (12)	0.0036 (12)

N2A	0.0129 (14)	0.0135 (14)	0.0176 (14)	0.0017 (11)	0.0055 (11)	0.0043 (11)
N3A	0.0154 (16)	0.0149 (14)	0.0200 (15)	0.0059 (12)	0.0039 (12)	0.0028 (12)
N4A	0.0167 (16)	0.0170 (15)	0.0213 (15)	0.0013 (12)	0.0110 (13)	0.0090 (12)
C1A	0.0207 (19)	0.0145 (17)	0.0153 (16)	−0.0010 (14)	0.0062 (14)	0.0039 (14)
C2A	0.0178 (18)	0.0184 (18)	0.0181 (17)	−0.0013 (14)	0.0078 (14)	0.0009 (14)
C3A	0.0165 (18)	0.0183 (18)	0.0246 (18)	0.0046 (15)	0.0074 (15)	0.0024 (15)
C4A	0.0148 (17)	0.0179 (17)	0.0200 (17)	0.0020 (14)	0.0072 (14)	0.0066 (14)
C5A	0.0131 (17)	0.0116 (16)	0.0138 (15)	0.0004 (13)	0.0027 (13)	0.0034 (13)
C6A	0.0133 (17)	0.0128 (16)	0.0143 (16)	0.0018 (13)	0.0044 (13)	0.0010 (13)
C7A	0.0128 (17)	0.0139 (16)	0.0157 (16)	0.0034 (13)	0.0022 (13)	0.0039 (13)
C8A	0.0165 (17)	0.0117 (15)	0.0108 (15)	0.0026 (13)	0.0029 (13)	0.0006 (13)
C9A	0.0125 (17)	0.0159 (16)	0.0117 (15)	0.0013 (13)	0.0023 (13)	0.0006 (13)
C10A	0.0140 (17)	0.0125 (16)	0.0144 (16)	0.0013 (13)	−0.0007 (13)	0.0010 (13)
C11A	0.0147 (17)	0.0101 (15)	0.0166 (16)	0.0002 (13)	0.0021 (13)	0.0017 (13)
C12A	0.0142 (17)	0.0164 (17)	0.0222 (18)	0.0017 (14)	0.0042 (14)	0.0032 (14)
C13A	0.0161 (18)	0.0146 (17)	0.034 (2)	0.0026 (14)	0.0048 (16)	−0.0006 (16)
C14A	0.0153 (18)	0.0150 (17)	0.040 (2)	0.0062 (15)	0.0020 (16)	0.0058 (16)
C15A	0.0208 (19)	0.0152 (17)	0.0275 (19)	0.0054 (15)	0.0019 (15)	0.0074 (15)
C16A	0.0183 (18)	0.0145 (16)	0.0124 (15)	0.0067 (14)	0.0080 (13)	0.0025 (13)
C17A	0.0163 (18)	0.0210 (18)	0.0139 (16)	0.0072 (14)	0.0060 (13)	0.0060 (14)
C18A	0.024 (2)	0.0209 (18)	0.0162 (17)	0.0097 (15)	0.0093 (15)	0.0077 (14)
C19A	0.0199 (18)	0.0161 (17)	0.0150 (16)	0.0079 (14)	0.0079 (14)	0.0046 (13)
C20A	0.024 (2)	0.0208 (18)	0.0193 (17)	0.0085 (16)	0.0065 (15)	0.0079 (15)
C21A	0.022 (2)	0.030 (2)	0.0147 (17)	0.0101 (16)	0.0020 (14)	0.0034 (15)
C22A	0.0174 (18)	0.0178 (17)	0.0172 (17)	0.0001 (14)	0.0031 (14)	0.0013 (14)
C23A	0.0193 (18)	0.0127 (16)	0.0148 (16)	0.0049 (14)	0.0044 (14)	0.0011 (13)
C24A	0.0162 (17)	0.0149 (16)	0.0074 (14)	0.0039 (13)	0.0046 (12)	−0.0018 (13)
N1B	0.0165 (15)	0.0167 (15)	0.0160 (14)	0.0083 (12)	0.0067 (12)	0.0066 (12)
N2B	0.0151 (15)	0.0131 (14)	0.0135 (13)	0.0037 (11)	0.0043 (11)	0.0018 (11)
N3B	0.0180 (16)	0.0228 (16)	0.0167 (15)	0.0078 (13)	0.0079 (12)	0.0091 (13)
N4B	0.0130 (15)	0.0207 (15)	0.0184 (14)	0.0022 (12)	0.0074 (12)	0.0076 (12)
C1B	0.0191 (18)	0.0204 (18)	0.0164 (16)	0.0061 (15)	0.0097 (14)	0.0090 (14)
C2B	0.0175 (18)	0.0237 (19)	0.0187 (17)	0.0054 (15)	0.0093 (14)	0.0041 (15)
C3B	0.0155 (18)	0.0223 (18)	0.0186 (17)	0.0080 (15)	0.0044 (14)	0.0061 (15)
C4B	0.0171 (18)	0.0192 (17)	0.0125 (16)	0.0044 (14)	0.0030 (13)	0.0053 (14)
C5B	0.0162 (17)	0.0149 (16)	0.0093 (15)	0.0017 (14)	0.0036 (13)	0.0016 (13)
C6B	0.0136 (17)	0.0131 (16)	0.0113 (15)	0.0017 (13)	0.0044 (13)	0.0007 (13)
C7B	0.0132 (17)	0.0138 (16)	0.0167 (16)	0.0048 (13)	0.0079 (13)	0.0029 (13)
C8B	0.0141 (17)	0.0129 (16)	0.0119 (15)	0.0013 (13)	0.0007 (13)	0.0041 (13)
C9B	0.0144 (17)	0.0164 (17)	0.0149 (16)	0.0013 (14)	0.0076 (13)	0.0019 (13)
C10B	0.0104 (16)	0.0134 (16)	0.0157 (16)	0.0031 (13)	0.0044 (13)	0.0012 (13)
C11B	0.0138 (17)	0.0128 (16)	0.0117 (15)	0.0005 (13)	0.0013 (13)	0.0011 (13)
C12B	0.0214 (19)	0.0167 (17)	0.0191 (17)	0.0071 (15)	0.0106 (14)	0.0084 (14)
C13B	0.0181 (19)	0.0216 (18)	0.0225 (18)	0.0086 (15)	0.0071 (15)	0.0037 (15)
C14B	0.025 (2)	0.026 (2)	0.027 (2)	0.0140 (17)	0.0067 (16)	0.0111 (16)
C15B	0.024 (2)	0.027 (2)	0.0242 (19)	0.0124 (16)	0.0076 (15)	0.0147 (16)
C16B	0.0170 (17)	0.0113 (15)	0.0128 (15)	0.0065 (13)	0.0055 (13)	0.0014 (13)
C17B	0.0151 (17)	0.0174 (17)	0.0157 (16)	0.0037 (14)	0.0031 (13)	0.0056 (14)

C18B	0.025 (2)	0.0153 (17)	0.0164 (17)	0.0064 (15)	0.0086 (15)	0.0063 (14)
C19B	0.0164 (18)	0.0140 (16)	0.0137 (16)	0.0040 (14)	0.0050 (13)	0.0028 (13)
C20B	0.024 (2)	0.0238 (19)	0.0136 (16)	0.0110 (16)	0.0061 (14)	0.0089 (14)
C21B	0.0171 (18)	0.0253 (19)	0.0145 (16)	0.0075 (15)	−0.0005 (14)	0.0013 (15)
C22B	0.0168 (18)	0.0196 (18)	0.0183 (17)	0.0024 (14)	0.0065 (14)	0.0015 (14)
C23B	0.0188 (18)	0.0146 (16)	0.0141 (16)	0.0075 (14)	0.0065 (14)	0.0025 (13)
C24B	0.0149 (17)	0.0105 (15)	0.0119 (15)	0.0049 (13)	0.0048 (13)	0.0005 (12)
O1W	0.0223 (14)	0.0228 (13)	0.0170 (12)	0.0058 (11)	0.0055 (10)	0.0080 (10)

Geometric parameters (Å, º)

Zn1—Cl14	2.2478 (9)	C21A—H21A	0.9300
Zn1—Cl11	2.2537 (9)	C22A—C23A	1.365 (5)
Zn1—Cl12	2.2935 (9)	C22A—H22A	0.9300
Zn1—Cl13	2.3098 (10)	C23A—C24A	1.408 (5)
Zn2—Cl24	2.2709 (9)	C23A—H23A	0.9300
Zn2—Cl21	2.2743 (9)	N1B—C1B	1.339 (4)
Zn2—Cl22	2.2809 (9)	N1B—C5B	1.353 (4)
Zn2—Cl23	2.2885 (9)	N1B—H1NB	0.848 (10)
Zn3—Cl34	2.2485 (10)	N2B—C6B	1.330 (4)
Zn3—Cl31	2.2713 (9)	N2B—C10B	1.347 (4)
Zn3—Cl33	2.2854 (9)	N3B—C15B	1.342 (4)
Zn3—Cl32	2.2981 (9)	N3B—C11B	1.353 (4)
N1A—C1A	1.337 (4)	N3B—H3NB	0.845 (10)
N1A—C5A	1.352 (4)	N4B—C18B	1.327 (4)
N1A—H1NA	0.851 (10)	N4B—C17B	1.358 (4)
N2A—C6A	1.327 (4)	N4B—H4NB	0.847 (10)
N2A—C10A	1.344 (4)	C1B—C2B	1.366 (5)
N3A—C15A	1.337 (4)	C1B—H1B	0.9300
N3A—C11A	1.351 (4)	C2B—C3B	1.377 (5)
N3A—H3NA	0.850 (10)	C2B—H2B	0.9300
N4A—C18A	1.321 (4)	C3B—C4B	1.392 (5)
N4A—C17A	1.367 (4)	C3B—H3B	0.9300
N4A—H4NA	0.846 (10)	C4B—C5B	1.382 (4)
C1A—C2A	1.370 (5)	C4B—H4B	0.9300
C1A—H1A	0.9300	C5B—C6B	1.475 (4)
C2A—C3A	1.394 (5)	C6B—C7B	1.396 (4)
C2A—H2A	0.9300	C7B—C8B	1.391 (4)
C3A—C4A	1.385 (5)	C7B—H7B	0.9300
C3A—H3A	0.9300	C8B—C9B	1.389 (4)
C4A—C5A	1.378 (4)	C8B—C16B	1.485 (4)
C4A—H4A	0.9300	C9B—C10B	1.399 (4)
C5A—C6A	1.485 (4)	C9B—H9B	0.9300
C6A—C7A	1.391 (4)	C10B—C11B	1.479 (4)
C7A—C8A	1.386 (4)	C11B—C12B	1.373 (4)
C7A—H7A	0.9300	C12B—C13B	1.386 (5)
C8A—C9A	1.393 (4)	C12B—H12B	0.9300
C8A—C16A	1.493 (4)	C13B—C14B	1.380 (5)

C9A—C10A	1.393 (4)	C13B—H13B	0.9300
C9A—H9A	0.9300	C14B—C15B	1.370 (5)
C10A—C11A	1.475 (4)	C14B—H14B	0.9300
C11A—C12A	1.385 (5)	C15B—H15B	0.9300
C12A—C13A	1.393 (5)	C16B—C17B	1.369 (5)
C12A—H12A	0.9300	C16B—C24B	1.431 (4)
C13A—C14A	1.372 (5)	C17B—H17B	0.9300
C13A—H13A	0.9300	C18B—C19B	1.393 (5)
C14A—C15A	1.364 (5)	C18B—H18B	0.9300
C14A—H14A	0.9300	C19B—C20B	1.414 (4)
C15A—H15A	0.9300	C19B—C24B	1.427 (4)
C16A—C17A	1.353 (5)	C20B—C21B	1.362 (5)
C16A—C24A	1.430 (4)	C20B—H20B	0.9300
C17A—H17A	0.9300	C21B—C22B	1.402 (5)
C18A—C19A	1.399 (5)	C21B—H21B	0.9300
C18A—H18A	0.9300	C22B—C23B	1.371 (5)
C19A—C20A	1.410 (5)	C22B—H22B	0.9300
C19A—C24A	1.422 (4)	C23B—C24B	1.411 (4)
C20A—C21A	1.367 (5)	C23B—H23B	0.9300
C20A—H20A	0.9300	O1W—H1WA	0.891 (10)
C21A—C22A	1.408 (5)	O1W—H1WB	0.893 (10)

Cl14—Zn1—Cl11	111.40 (4)	C23A—C22A—H22A	119.4
Cl14—Zn1—Cl12	108.56 (4)	C21A—C22A—H22A	119.4
Cl11—Zn1—Cl12	113.15 (3)	C22A—C23A—C24A	120.5 (3)
Cl14—Zn1—Cl13	110.21 (4)	C22A—C23A—H23A	119.8
Cl11—Zn1—Cl13	108.22 (3)	C24A—C23A—H23A	119.8
Cl12—Zn1—Cl13	105.10 (3)	C23A—C24A—C19A	118.1 (3)
Cl24—Zn2—Cl21	107.85 (3)	C23A—C24A—C16A	124.3 (3)
Cl24—Zn2—Cl22	110.83 (3)	C19A—C24A—C16A	117.6 (3)
Cl21—Zn2—Cl22	112.43 (3)	C1B—N1B—C5B	123.4 (3)
Cl24—Zn2—Cl23	108.03 (3)	C1B—N1B—H1NB	118 (2)
Cl21—Zn2—Cl23	109.70 (3)	C5B—N1B—H1NB	119 (2)
Cl22—Zn2—Cl23	107.91 (3)	C6B—N2B—C10B	117.8 (3)
Cl34—Zn3—Cl31	108.35 (4)	C15B—N3B—C11B	123.2 (3)
Cl34—Zn3—Cl33	113.83 (4)	C15B—N3B—H3NB	118 (2)
Cl31—Zn3—Cl33	108.80 (4)	C11B—N3B—H3NB	119 (2)
Cl34—Zn3—Cl32	113.05 (4)	C18B—N4B—C17B	122.5 (3)
Cl31—Zn3—Cl32	110.43 (3)	C18B—N4B—H4NB	119 (2)
Cl33—Zn3—Cl32	102.23 (3)	C17B—N4B—H4NB	119 (2)
C1A—N1A—C5A	123.4 (3)	N1B—C1B—C2B	120.0 (3)
C1A—N1A—H1NA	116 (2)	N1B—C1B—H1B	120.0
C5A—N1A—H1NA	120 (2)	C2B—C1B—H1B	120.0
C6A—N2A—C10A	118.2 (3)	C1B—C2B—C3B	119.0 (3)
C15A—N3A—C11A	123.4 (3)	C1B—C2B—H2B	120.5
C15A—N3A—H3NA	117 (2)	C3B—C2B—H2B	120.5
C11A—N3A—H3NA	119 (2)	C2B—C3B—C4B	120.0 (3)
C18A—N4A—C17A	122.5 (3)	C2B—C3B—H3B	120.0

C18A—N4A—H4NA	115 (2)	C4B—C3B—H3B	120.0
C17A—N4A—H4NA	123 (2)	C5B—C4B—C3B	119.9 (3)
N1A—C1A—C2A	120.6 (3)	C5B—C4B—H4B	120.1
N1A—C1A—H1A	119.7	C3B—C4B—H4B	120.1
C2A—C1A—H1A	119.7	N1B—C5B—C4B	117.7 (3)
C1A—C2A—C3A	117.9 (3)	N1B—C5B—C6B	116.9 (3)
C1A—C2A—H2A	121.0	C4B—C5B—C6B	125.3 (3)
C3A—C2A—H2A	121.0	N2B—C6B—C7B	123.5 (3)
C4A—C3A—C2A	120.1 (3)	N2B—C6B—C5B	116.0 (3)
C4A—C3A—H3A	119.9	C7B—C6B—C5B	120.5 (3)
C2A—C3A—H3A	119.9	C8B—C7B—C6B	118.9 (3)
C5A—C4A—C3A	120.1 (3)	C8B—C7B—H7B	120.6
C5A—C4A—H4A	119.9	C6B—C7B—H7B	120.6
C3A—C4A—H4A	119.9	C9B—C8B—C7B	117.9 (3)
N1A—C5A—C4A	117.8 (3)	C9B—C8B—C16B	121.4 (3)
N1A—C5A—C6A	116.1 (3)	C7B—C8B—C16B	120.7 (3)
C4A—C5A—C6A	126.0 (3)	C8B—C9B—C10B	119.5 (3)
N2A—C6A—C7A	122.9 (3)	C8B—C9B—H9B	120.2
N2A—C6A—C5A	115.7 (3)	C10B—C9B—H9B	120.2
C7A—C6A—C5A	121.3 (3)	N2B—C10B—C9B	122.3 (3)
C8A—C7A—C6A	119.1 (3)	N2B—C10B—C11B	116.6 (3)
C8A—C7A—H7A	120.4	C9B—C10B—C11B	121.1 (3)
C6A—C7A—H7A	120.4	N3B—C11B—C12B	118.3 (3)
C7A—C8A—C9A	118.3 (3)	N3B—C11B—C10B	116.2 (3)
C7A—C8A—C16A	120.5 (3)	C12B—C11B—C10B	125.5 (3)
C9A—C8A—C16A	121.1 (3)	C11B—C12B—C13B	119.6 (3)
C8A—C9A—C10A	118.7 (3)	C11B—C12B—H12B	120.2
C8A—C9A—H9A	120.7	C13B—C12B—H12B	120.2
C10A—C9A—H9A	120.7	C14B—C13B—C12B	120.4 (3)
N2A—C10A—C9A	122.7 (3)	C14B—C13B—H13B	119.8
N2A—C10A—C11A	115.6 (3)	C12B—C13B—H13B	119.8
C9A—C10A—C11A	121.7 (3)	C15B—C14B—C13B	118.7 (3)
N3A—C11A—C12A	118.1 (3)	C15B—C14B—H14B	120.6
N3A—C11A—C10A	116.2 (3)	C13B—C14B—H14B	120.6
C12A—C11A—C10A	125.8 (3)	N3B—C15B—C14B	119.7 (3)
C11A—C12A—C13A	119.0 (3)	N3B—C15B—H15B	120.2
C11A—C12A—H12A	120.5	C14B—C15B—H15B	120.2
C13A—C12A—H12A	120.5	C17B—C16B—C24B	119.1 (3)
C14A—C13A—C12A	120.5 (3)	C17B—C16B—C8B	118.4 (3)
C14A—C13A—H13A	119.7	C24B—C16B—C8B	122.5 (3)
C12A—C13A—H13A	119.7	N4B—C17B—C16B	120.7 (3)
C15A—C14A—C13A	119.0 (3)	N4B—C17B—H17B	119.6
C15A—C14A—H14A	120.5	C16B—C17B—H17B	119.6
C13A—C14A—H14A	120.5	N4B—C18B—C19B	120.6 (3)
N3A—C15A—C14A	120.0 (3)	N4B—C18B—H18B	119.7
N3A—C15A—H15A	120.0	C19B—C18B—H18B	119.7
C14A—C15A—H15A	120.0	C18B—C19B—C20B	120.4 (3)
C17A—C16A—C24A	119.7 (3)	C18B—C19B—C24B	118.9 (3)

C17A—C16A—C8A	118.2 (3)	C20B—C19B—C24B	120.6 (3)
C24A—C16A—C8A	122.0 (3)	C21B—C20B—C19B	120.0 (3)
C16A—C17A—N4A	120.6 (3)	C21B—C20B—H20B	120.0
C16A—C17A—H17A	119.7	C19B—C20B—H20B	120.0
N4A—C17A—H17A	119.7	C20B—C21B—C22B	119.8 (3)
N4A—C18A—C19A	120.3 (3)	C20B—C21B—H21B	120.1
N4A—C18A—H18A	119.8	C22B—C21B—H21B	120.1
C19A—C18A—H18A	119.8	C23B—C22B—C21B	121.6 (3)
C18A—C19A—C20A	120.5 (3)	C23B—C22B—H22B	119.2
C18A—C19A—C24A	119.1 (3)	C21B—C22B—H22B	119.2
C20A—C19A—C24A	120.4 (3)	C22B—C23B—C24B	120.5 (3)
C21A—C20A—C19A	119.8 (3)	C22B—C23B—H23B	119.7
C21A—C20A—H20A	120.1	C24B—C23B—H23B	119.7
C19A—C20A—H20A	120.1	C23B—C24B—C19B	117.4 (3)
C20A—C21A—C22A	120.0 (3)	C23B—C24B—C16B	124.7 (3)
C20A—C21A—H21A	120.0	C19B—C24B—C16B	117.9 (3)
C22A—C21A—H21A	120.0	H1WA—O1W—H1WB	106 (2)
C23A—C22A—C21A	121.2 (3)		

C5A—N1A—C1A—C2A	−0.7 (5)	C5B—N1B—C1B—C2B	1.6 (5)
N1A—C1A—C2A—C3A	−0.4 (5)	N1B—C1B—C2B—C3B	−1.6 (5)
C1A—C2A—C3A—C4A	1.3 (5)	C1B—C2B—C3B—C4B	0.5 (5)
C2A—C3A—C4A—C5A	−1.2 (5)	C2B—C3B—C4B—C5B	0.7 (5)
C1A—N1A—C5A—C4A	0.8 (5)	C1B—N1B—C5B—C4B	−0.4 (5)
C1A—N1A—C5A—C6A	178.6 (3)	C1B—N1B—C5B—C6B	179.9 (3)
C3A—C4A—C5A—N1A	0.1 (5)	C3B—C4B—C5B—N1B	−0.7 (5)
C3A—C4A—C5A—C6A	−177.4 (3)	C3B—C4B—C5B—C6B	179.0 (3)
C10A—N2A—C6A—C7A	0.8 (5)	C10B—N2B—C6B—C7B	0.5 (5)
C10A—N2A—C6A—C5A	−177.8 (3)	C10B—N2B—C6B—C5B	179.9 (3)
N1A—C5A—C6A—N2A	3.3 (4)	N1B—C5B—C6B—N2B	3.4 (4)
C4A—C5A—C6A—N2A	−179.1 (3)	C4B—C5B—C6B—N2B	−176.3 (3)
N1A—C5A—C6A—C7A	−175.3 (3)	N1B—C5B—C6B—C7B	−177.2 (3)
C4A—C5A—C6A—C7A	2.3 (5)	C4B—C5B—C6B—C7B	3.1 (5)
N2A—C6A—C7A—C8A	−0.5 (5)	N2B—C6B—C7B—C8B	2.7 (5)
C5A—C6A—C7A—C8A	178.0 (3)	C5B—C6B—C7B—C8B	−176.6 (3)
C6A—C7A—C8A—C9A	−0.1 (5)	C6B—C7B—C8B—C9B	−3.6 (5)
C6A—C7A—C8A—C16A	−177.0 (3)	C6B—C7B—C8B—C16B	177.4 (3)
C7A—C8A—C9A—C10A	0.4 (4)	C7B—C8B—C9B—C10B	1.5 (5)
C16A—C8A—C9A—C10A	177.3 (3)	C16B—C8B—C9B—C10B	−179.5 (3)
C6A—N2A—C10A—C9A	−0.5 (5)	C6B—N2B—C10B—C9B	−2.8 (5)
C6A—N2A—C10A—C11A	−179.5 (3)	C6B—N2B—C10B—C11B	−179.6 (3)
C8A—C9A—C10A—N2A	−0.1 (5)	C8B—C9B—C10B—N2B	1.8 (5)
C8A—C9A—C10A—C11A	178.9 (3)	C8B—C9B—C10B—C11B	178.5 (3)
C15A—N3A—C11A—C12A	0.3 (5)	C15B—N3B—C11B—C12B	−1.5 (5)
C15A—N3A—C11A—C10A	179.8 (3)	C15B—N3B—C11B—C10B	179.3 (3)
N2A—C10A—C11A—N3A	−6.5 (4)	N2B—C10B—C11B—N3B	4.3 (4)
C9A—C10A—C11A—N3A	174.5 (3)	C9B—C10B—C11B—N3B	−172.5 (3)
N2A—C10A—C11A—C12A	173.0 (3)	N2B—C10B—C11B—C12B	−174.8 (3)

C9A—C10A—C11A—C12A	−6.0 (5)	C9B—C10B—C11B—C12B	8.4 (5)
N3A—C11A—C12A—C13A	1.1 (5)	N3B—C11B—C12B—C13B	1.6 (5)
C10A—C11A—C12A—C13A	−178.3 (3)	C10B—C11B—C12B—C13B	−179.3 (3)
C11A—C12A—C13A—C14A	−1.1 (5)	C11B—C12B—C13B—C14B	−0.8 (5)
C12A—C13A—C14A—C15A	−0.3 (5)	C12B—C13B—C14B—C15B	−0.2 (5)
C11A—N3A—C15A—C14A	−1.8 (5)	C11B—N3B—C15B—C14B	0.5 (5)
C13A—C14A—C15A—N3A	1.8 (5)	C13B—C14B—C15B—N3B	0.4 (5)
C7A—C8A—C16A—C17A	130.7 (3)	C9B—C8B—C16B—C17B	−42.9 (4)
C9A—C8A—C16A—C17A	−46.1 (4)	C7B—C8B—C16B—C17B	136.1 (3)
C7A—C8A—C16A—C24A	−46.8 (4)	C9B—C8B—C16B—C24B	136.9 (3)
C9A—C8A—C16A—C24A	136.4 (3)	C7B—C8B—C16B—C24B	−44.1 (4)
C24A—C16A—C17A—N4A	1.1 (5)	C18B—N4B—C17B—C16B	2.9 (5)
C8A—C16A—C17A—N4A	−176.5 (3)	C24B—C16B—C17B—N4B	2.0 (5)
C18A—N4A—C17A—C16A	1.8 (5)	C8B—C16B—C17B—N4B	−178.2 (3)
C17A—N4A—C18A—C19A	−2.2 (5)	C17B—N4B—C18B—C19B	−4.2 (5)
N4A—C18A—C19A—C20A	179.9 (3)	N4B—C18B—C19B—C20B	−177.1 (3)
N4A—C18A—C19A—C24A	−0.2 (5)	N4B—C18B—C19B—C24B	0.6 (5)
C18A—C19A—C20A—C21A	178.7 (3)	C18B—C19B—C20B—C21B	177.2 (3)
C24A—C19A—C20A—C21A	−1.1 (5)	C24B—C19B—C20B—C21B	−0.4 (5)
C19A—C20A—C21A—C22A	−1.4 (5)	C19B—C20B—C21B—C22B	−1.1 (5)
C20A—C21A—C22A—C23A	1.3 (5)	C20B—C21B—C22B—C23B	0.6 (5)
C21A—C22A—C23A—C24A	1.4 (5)	C21B—C22B—C23B—C24B	1.4 (5)
C22A—C23A—C24A—C19A	−3.8 (5)	C22B—C23B—C24B—C19B	−2.8 (4)
C22A—C23A—C24A—C16A	177.2 (3)	C22B—C23B—C24B—C16B	177.8 (3)
C18A—C19A—C24A—C23A	−176.1 (3)	C18B—C19B—C24B—C23B	−175.3 (3)
C20A—C19A—C24A—C23A	3.7 (5)	C20B—C19B—C24B—C23B	2.3 (5)
C18A—C19A—C24A—C16A	2.9 (4)	C18B—C19B—C24B—C16B	4.1 (4)
C20A—C19A—C24A—C16A	−177.2 (3)	C20B—C19B—C24B—C16B	−178.3 (3)
C17A—C16A—C24A—C23A	175.7 (3)	C17B—C16B—C24B—C23B	174.0 (3)
C8A—C16A—C24A—C23A	−6.9 (5)	C8B—C16B—C24B—C23B	−5.8 (5)
C17A—C16A—C24A—C19A	−3.3 (4)	C17B—C16B—C24B—C19B	−5.4 (4)
C8A—C16A—C24A—C19A	174.1 (3)	C8B—C16B—C24B—C19B	174.8 (3)